Volume 1 | Number 1 | Jan 2013 | Pages 1–100

Nanoscale

www.rsc.org/nanoscale

ROYAL SOCIETY OF CHEMISTRY

ROYAL SOCIETY OF CHEMISTRY

www.rsc.org/nanoscale

ARTICLE TYPE

Superhydrophobic Nanocoatings: From Materials to Fabrications and to Applications

Yifan Si[a, b], and Zhiguang Guo[a,b*]

Superhydrophobic nanocoatings, a combination of nanotechnology and superhydrophobic surface, have received extraordinary attention recently, focusing both on novel preparation strategies and on investigations of their unique properties. In the past dedcades, inspired by lotus leaf, the discovery of nano- and micro- hierarchical structure has brought about great change in superhydrophobic nanocoatings
10 field. In this paper we review the contributions to this field reported in recent literatures, mainly including materials, fabrication and applications. In order to facilitate comparison, materials are divided into 3 categories as follow: the inorganic materials, the organic materials, and the inorganic-organic materials. But each kind of materials has itself merits and demerits, as well as fabrication techniques. The process of each technique is illustrated simply through a few classical examples. There is, to some extent, an
15 association between various fabrication techniques, but a more one is different. So, it is important to choose proper preparation strategies, according to condition and purposes. The peculiar properties of superhydrophobic nanocoatings, such as self-cleaning, anti-bacteria, anti-icing, corrosion resistance and so on, are the most dramatic. Not only do we introduce the application instances, but also try to superficial expound the principle behind the phenomenon. Finally, some challenges and the potential
20 promising breakthroughs are also succinctly highlighted in this field.

Introduction

As a result of the development of nanotechnology, science reform sparkle world widely since beginning of 21st century. So, fast-
25 evolving world of nanotechnology captivates researchers in field ranging from industry, agriculture to military.[1-3] A more generalized description of nanotechnology was subsequently established by the National Nanotechnology Initiative, which defines nanotechnology as the manipulation of matter with at
30 least one dimension sized from 1 to 100 nanometers. At the same time, the features of bio-inspired superhydrophobic surfaces have aroused worldwide interest during the past few years duo to their peculiar properties and potential applications.[4-7] It is particularly worth mentioning here that "superhydrophobic surfaces" have
35 been ranked the 7th in Top 20 research fronts in materials science during 2006 and 2010 from Essential Science indicators database.[8] Most important of all, superhydrophobic nanocoatings cover nanotechnology and superhydrophobic surface together. Superhydrophobic nanocoatings can be defined as one kind of
40 superhydrophobic coating which includes at least one nanoscaled raw material that play a vital role to coating's property, or the morphology of the superhydrophobic coating is nanoscale in a certain dimension.

The methods used for surface modification on substrates
45 directly such as etching, lithography, are quite limited. And the range of substrates is restricted for the properties of substrate place certain guidelines to satisfy experiment requirement. There is no doubt that coating is one of the best ways to change solid surface properties. Different from "surface modification directly",
50 coating is regarded as indirect modification method through chemical or physical process to "create" a layer of new substances with totally different properties on the substrate surface as protective or multifunction layer. Based on this point, the range of, no matter materials or fabrication methods of
55 surface modification, has increased immediately. As one kind of emerging nanomaterial, superhydrophobic nanocoating, an important method in surface superhydrophobization with marvelous effects, has aroused dramatic change in surface and interfacial research field. In fact, as a wise mentor of humans,
60 nature has vast biological surface exhibiting superhydrophobicity including lotus leaves[9], the gecko feet[24], the Namib desert beetle[25] and water strider[26] for a very long time. Certainly, as diligent students, researchers have been working hard to find out various smart methods for attaining superhydrophobic
65 nanocoatings. In consideration of the particularity of nanocoatings, so when talk about fabrication, some new affecting factors, like the reserve of nanoscale roughness, the thickness of coating, mechanical stability, and binding strength between the coating and the substrate, should be noted.

70 The unique way in which the nanoscale roughness interplay with liquids makes them a promising platform for many

applications in the field of superhydrophobic nanocoating as mentioned in some excellent literatures, such as self-cleaning, anti-bacteria, anti-icing, corrosion resistance and so on.[21-23, 31] Both of them would be discussed detailedly in the following.

5 Functional superhydrophobic nanocoatings can solve lots of problems of real life. Just because of this, the researchers' efforts to this aspect can be said arduous and rewarding. Remarkably, the definition of nanocoating is not in conformity with the traditional nanomaterial completely, and so far, the concept of 10 superhydrophobic nanocoating is not well known. So, many researches did not point out this concept directly in their works. However, the research works of this part cannot be neglected.

Surface wetting behavior, generally, can be divided into 4 different regimes according to the water contact angle (WCA). 15 Hydrophilic and hydrophobic regimes, defined as WCA in the range of $10° < \theta < 90°$ and $90° < \theta < 150°$ respectively, are the most conventional regimes. Superhydrophilic and superhydrophobic regimes are more interesting for the extremes of surface wetting behavior with WCA in the range of $0° < \theta < 10°$ 20 and $150° < \theta < 180°$ respectively.[20] The most notable one, superhydrophobic regime, describes a state of nearly perfect non-wetting. On the other hand, superhydrophobic surfaces exhibit extremely low water contact angle hysteresis (CAH) (< 10°) that result in the rolling of the water droplets easily.[4] It is well known 25 that lotus leaf let us recognize at the superhydrophobicity in nature.[9, 29] It took some further decades to resolve the mechanism behind this phenomenon but without much success until the introduction of scanning electron microscopy (SEM). By the virtue of a SEM, it is found that the surfaces of lotus leaves 30 shows protruding nubs of 20–40 μm apart each covered with a smaller scale rough of epicuticular wax crystalloids. Jiang et al. [10] reported that the nanoscaled roughness endowed surface superhydrophobicity with a large fraction of air, which is the first example for nanostructure based superhydrophobicity. After a 35 series of studies and endeavor of many researchers[11-16], they found that micro-nanoscale hierarchical structures, rather than individual micrometer scaled model, can indeed attribute to steady superhydrophobic surfaces. In fact, for rough surface, seeking to understand the relationship between surface roughness 40 and superhydrophobicity, Wenzel's and Cassie's[17, 18] models are established and applied from long time ago. These two models describe different wetting state and supply theoretical guidance for us. Low surface energy materials[19, 27, 32], such as – CF$_3$ groups, silyl compound, or fluorocarbons, are another necessary factors 45 for preparing superhydrophobic surfaces inspired by the epicuticular wax crystalloids of lotus leaf. Similarly, the great amount of study had been applied in this aspect.

In this review, we first briefly introduce the fundamental theory aspects on surface wetting property, mainly focusing on 50 superhydrophobicity in air. On the basis of this understanding, in the following sections, we will cover the materials, fabrications and applications of superhydrophobic nanocoatings. In Section 3, we classified materials into 3 categories in comparison. Recently developed fabrication techniques and applications have been 55 discussed as well. In order to keep up with the forefront of this research field, we will try to be concerned with the research works of last four years. We also highlight a few new methodologies and potential applications. Finally, we briefly

present our personal view of the open questions, remaining 60 challenges and development tendency of this field.

Fundamental theories

Smooth surface

It is well know that atoms or molecules at the surface of solid or liquids have higher energy because of the fewer bonds with 65 neighboring atoms than interior atoms or molecules, which results in surface tension, or surface energy, measured in N/m. when liquid drops placed in contact with a solid surface, it tend to reach stable state with relatively lower energy. So, there is a contact angle measured at the edge of droplet (Fig. 1a). CA (θ) is 70 an important parameter for characterizing the surface wettability described by the Young Eq. (1) [33]:

$$\cos \theta = \frac{(\gamma_{SV} - \gamma_{SL})}{\gamma_{LV}} \tag{1}$$

where γ_{SV}, γ_{SL} and γ_{LV} are the surface tension at solid–vapor (gas), solid–liquid, and liquid–vapor (gas) interfaces, respectively. 75 For contact angles less than 90°, the surface is conventionally called as hydrophilic, if the contact angle varies between 90° and 150°, the surface is hydrophobic, and if water contact angle is greater than 150°, the surface is described as superhydrophobic. However, this equation is applicable only to smooth surfaces. As 80 to rough ones, the theories need to be modified.

Rough surface

In order to explain the effect of roughness on the apparent contact angle of a liquid droplet on a solid surface, two classical well-established models for describing the roughness-induced 85 wettability have been developed by Wenzel[17] and Cassie and Baxter [18].

In 1936, Wenzel took surface roughness into the theoretical study for the first time. Based on comprehensive considerations of influence of roughness on wettability, Wenzel proposed a new 90 model, called Wenzel model (Fig. 1b). This model can be used to describe the contact angle in this situation that the liquid is in contact with the entire solid surface and completely penetrates into cavities. He modified the Young equation as follows:

$$\cos \theta_w = r \cos \theta \tag{2}$$

95 It is explicit that a rough material has higher surface area than a smooth one according to Wenzel model and the surface area is associated with roughness factor r,

$$r = \text{roughness} = \frac{\text{actual surface}}{\text{geometric surface}} \tag{3}$$

As a result, when $\theta < 90°$, an increasing r will reduce θ_w, but if 100 $\theta > 90°$, an increasing in roughness leads to an increase in θ_w.

Wenzel equation is only valid for the homogeneous wetting regime, however, the liquid drop cannot penetrate into cavities on the rough surface in all cases and the air is trapped in these cavities, which lead to a composite interface.

105 In 1944, Cassie and Baxter proposed the following equation for this model:

$$\cos \theta_{CB} = f_{SL} \cos \theta_1 + f_{LV} \cos \theta_2 \qquad (4)$$

Heterogeneous surfaces composed of two fractions, shown in Fig. 1c, the first fraction corresponds to the solid-liquid interface ($\cos \theta_1 = \cos \theta$) and the second fraction to the liquid–air interface ($f_{SL} = 1 - f_{LV}$; $\theta_2 = 180°$). So the equation becomes:

$$\cos \theta_{CB} = f_{SL}(1 + \cos \theta_w) - 1 \qquad (5)$$

As a matter of fact, Wenzel equation and Cassie-Baxter equation describe two limit behaviors. A mixed model (Fig. 1d)[34] was introduced by Marmur. In this model, surface may show intermediate state that a droplet partially wets the surface and partially sits on air pockets. The apparent contact angle depends on both solid solid-surface fraction f and roughness factor r. The equation that describes this situation is the following:

$$\cos \theta^* = r_f f_{SL} \cos \theta + f_{SL} - 1 \qquad (6)$$

where r_f the roughness of the portion of the solid that touches the liquid. When $f_{SL} = 1$, $r_f = r$, Eq. (6) turns into Eq. (2).

Generally speaking, surfaces that are wetted in the Wenzel state are usually sticky, while surface in the Cassie-Baxter state are slippery. In real life, it is likely that Cassie-Baxter state transform into Wenzel state under the conditions of droplet press, impact or vibration. Frankly, there are still some challenges for these two models to explain real conditions between droplets and solid surfaces. But what we know is surface roughness and chemical compositions both play key roles in the contact angle of a liquid droplet on a solid surface.
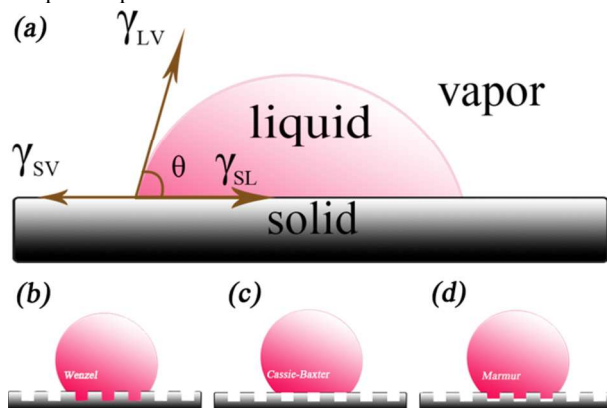
Fig. 1 Liquid droplet on a rough surface (a). Behavior of a liquid droplet on a rough surface, Wenzel state (b); Cassie-Baxter state (c); Marmur state (d).

Dynamic wettability

No matter Wenzel equation or Cassie-Baxter equation all could only predict the apparent CA in the equilibrium state, describing the behavior of a state liquid drop. But under the actual situation, CA is not enough to characterize the wetting properties of a solid-liquid interface, such as dynamic wettability. With the farther investigations, researchers have put forward the concept of contact angle hysteresis and sliding angle (SA) to solve this problem. When a droplet is inflated, the CA will increase but the contact area not change until θ_{adv} reaches a critical value and then it begins to advance. θ_{adv} is referred to as the advancing angle. Similarly, if a droplet is deflated, there also is a critical

value called receding angle θ_{rec} until the droplet begins to recede. By definition, the difference between advancing and receding CA is termed CAH. As to SA, it can be measured as an inclined plate tilts at a critical angle, beyond which a liquid drop will roll off the plate surface. Surface with low hysteresis allow drops to slide over them easily whatever the equilibrium contact angle, the quantitative relationship between the CAH and SA is provided by eq.(7)[35]:

$$mg \sin \alpha = \gamma_{LV} w (\theta_{rec} - \theta_{adv}) \qquad (7)$$

where θ_{adv} and θ_{rec} are the advancing and receding angles, respectively, g is the gravity force, and m and w represent the mass and width of the drop, respectively. Essentially, this equation is the equality of gravity force and capillary force. It can draw the conclusion that the Cassie-Baxter model will result in a smaller SA than Wenzel model because of the less area fraction of the liquid droplet in contact with the solid surface.

The role of nanoscale roughness

As mentioned in the previous section, two factors, surface roughness and chemical compositions, influence the surface wettability together. Meanwhile, note that the maximum contact angle of a water droplet reported on a lowest-energy smooth surface is about 130°.[36-37] In other words, there is a limit as to how much surface energy can affect the surface wettability. Roughness seems to be a much more remarkable and complex principal factor. In 1997, inspired by lotus, the SEM image of lotus leaf (Nelumbo nucifera) has shown fine-branched nanostructures on top of microsized papillae. Barthlott and Neinhuis'[38-39] early work has started the recent research that used micro-nanoscale hierarchical structure to explain the surface extreme repellence against liquid droplets. They also coined the term "lotus effect" for this property and pointed the way towards how to mimic the nature. Following researchers has conducted a significant amount of research on micro-nanoscale hierarchical.[40-42] It turned out that micro-nanoscale hierarchical is more conductive to the Cassie-Baxter state with high CA and low SA. Nanocoating is easy to construct nanoscale roughness owing to the existence of nanoscale raw materials. With further low-energy treatment, superhydrophobic nanocoating is achieved. Thus it can be seen that, in regard to suphydrophobic nanocoating, there are strong and comprehensive theoretical supports.

Materials for nanocoatings

Materials, a key to structure nano-micro hierarchical roughness, always play decisive roles for the properties of superhydrophobic nanocoatings. In order to show references information clearly and roundly, the applied materials for surperhydrophobic nanocoating are divided into three categories embracing the inorganic materials, the organic materials, and the inorganic-organic materials (see summary in Table 1) from the papers published in recent years, in which the "materials" mean what play the core role in the fabrication process, chemical component or structure of corresponding nanocoatings.

Inorganic materials

Silica-based

It is well known that silica-based materials act as the most common choices in biomimetic superhydrophobic nanocoating area.[43-50] In fact, silica-based materials are intrinsically hydrophilic, but they are also convenient further chemical treatment to obtain superhydrophobicity. At the same time, the excellent optical property of silica-based materials is another advantage.

For example, Yazdanshenas and Shateri-Khalilabad[43] developed a facile one-step ultrasound-assisted approach using tetraethylorthosilicate (TEOS) and octyltriethoxysilane (OTES) for the synthesis of silica nanoparticles functionalized superhydrophobic nanocoating on cotton fabrics. Zhang et al.[44] made a superhydrophobic RTV silicone rubber coating via common methods such as spray, brush and dip coating using fluoric nanoparticles and silicone rubber. This nanocoating has CA higher than 145° and good UV durability. Similarly, through spraying the mixture of silicone rubber coating, Zeng et al.[45] prepared superhydrophobic nanocoating which showed hierarchical roughness with a water CA of 153°. Interestingly, with the increase in calcination temperature from 100 °C to 400 °C, the superhydrophobic PDMS/SiO₂ coating became transparent with the visible light transmittance increasing from 40% to 80%, but when the calcination temperature was over 500 °C, the wetting behavior of the coating changed from superhydrophobicity to superhydrophilicity with a WCA of nearly 0°. Inspired by nepenthes pitcher, Zhang's group[46] reported a fabrication of fluoro-SNs/Krytox by the combination of fluoro-silicone nanofilaments (fluoro-SNs) and Krytox liquids, perfluoropolyethers. Unlike the lotus-inspired superhydrophobic coating, the sliding speed of liquid drops is obviously slower on this coating because of influence of microstructure of fluoro-SNs, properties of the Krytox layer (e.g., thickness and viscosity) and tilting angle.

Of course it is not perfect, how to improve the mechanical stability and robustness of silica-based superhydrophobic nanocoating is the issue that scientists concern now.

Carbon-based

With the discovery of some novel carbon materials, such as carbon nanotube (CNT), carbon nanofiber (CNF), grapheme and Fullerene-C, carbon-based materials has come to be a hot focus in many fields including superhydrophobic nanocoating area. The mechanical and chemical stability and robustness of carbon-based materials need not worry for the strong stability of carbon itself. But how to design nano rougness in a certain dimension would be a nerve-wracking trouble.

For example, it is difficult to achieve the structural hierarchy of two-dimensional grapheme for superhydrophobicity. However, Park and co-workers reported an ingenious route to solve this puzzle.[51] They obtained graphene/Nafion nanohybrid films (Fig. 2a) by controlling the structures with respect to the chemical composition to achieve the hierarchical petal-like, porous structure (surface area of 413.46 m² g⁻¹). Such a surface exhibited a superhydrophobicity with WCA of ∼ 161°. Jang et al.[52] presented another simple route toward a superhydrophobic grapheme surface via thermal reduction method. By reduction of grapheme oxide and removal of silica particle, researchers obtained a transparent nano-sphere structure (Fig. 2b) with a high water contact angle. The excellent properties of transparent superhydrophobic graphene can potentially be exploited for versatile applications. Comparing with graphene, using CNT to fabricate superhydrophobic nanocoating would be easier. Men et al.[53] papered a superhydrophobic nanocoating by spraying multiwall carbon nanotubes (CNTs) onto substrates followed by surface fluorination. WCA of this coating came up to 163°. Han et al.[54] fabricated anti-frost coatings containing carbon nanotube composite with reliable thermal cyclic property by spraying process as well. Furthermore, the study showed that the nanoporous structure of superhydrophobic coatings was of great importance for both wettability and mechanical reliability. The high price of nano carbon-based materials are the biggest obstacle for large-scale preparation, so it seems that the research of the part still stay in the laboratory.
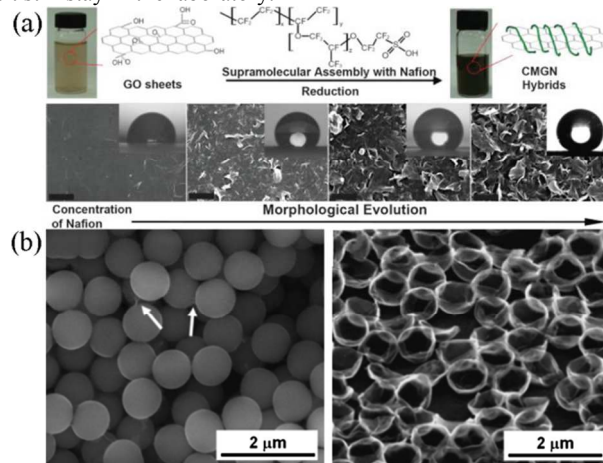
Fig. 2 (a) Illustration of a procedure to fabricate CMGNs through supramolecular assembly (top panel) and structural transition of hybrid films with respect to the chemical composition of Nafion, as shown in SEM images (bottom panel). Scale bars are 1 μm. The inset of the bottom panel is the CA photography of CMGN films.[51] (b) SEM images of the samples: Left, GO/NH₂–SiO₂. Envelopes of SiO₂ by GO sheets are apparent in the regions indicated by white arrows. Right, GO-nanospheres after removal of SiO₂ in HF solution. Some outlets were found due to rupture of the spheres during exhaust of evolved gas.[52] (a) Reproduced with permission from [51], Copyright (2012) The Royal Society of Chemistry. (b) Reproduced with permission from [52], Copyright (2013) The Royal Society of Chemistry.

Metallic

Generally, metallic superhydrophobic nanocoating is obtained always by electrochemical processes. Regan and Chapman[55] described a novel preparation for superhydrophobic nanofunctioanal silver and gold on copper substrates using an electroless galvanic reaction between copper and metal salt (silver chloride and gold chloride). These copper-coated substrates could be potential antifouling coatings for environmental monitoring devices. Through electrodeposition techniques, Liang et al.[56] prepared nickel coating with micro-nano binary structure. Followed by a fluorinated modification process to obtain superhydrophobicity, the WCA with 5 μL water droplets on the nickel film after fluorinated modification is higher than 160°, and the sliding angle with 10 μL water droplets is as low as 1°. What is more, this film has satisfied stability both in strong acid and alkaline solutions, and can keep superhydrophobicity more than 400 days under ambient conditions. With the same method, superhydrophobic Ni-Co alloy coating with hierarchical flowerlike structures was reported[57] with a water CA as high as 167.3 ± 1.3° and an ultra-low sliding

angle of about 1° as well.

Objectively speaking, superhydrophobic nanocoating is necessary of the protection of metal, but it is hard to use metal as a coating. So, instances of metallic material superhydrophobic nanocaoting are few in number.

Metallic oxide

Comparing to metallic superhydrophobic nanocoating, there are a larger number and more kinds of metallic oxide examples in this field. Low temperature plasma method have been utilized by Borras et al.[58] to fabricate Ag@TiO$_2$ core@shell nanorods (Fig. 3a) superhydrophobic nanocoating on silver covered Si (100) wafer substrates. Such coating would turn into superhydrophilic by irradiation with UV light because of TiO$_2$ transforms into superhydrophilic. Deng et al.[59] obtained one kind of hierarchical alumina pyramids-on-pores (HAPOP) rough structure (Fig. 3b) by high effective one-step anodization process. Subsequently modified with low-surface energy agent, no matter 1H, 1H, 2H, 2H-perfluorodecyltriethoxysilor (PDES) or stearic acid (STA), this film became superhydrophobic with a series of superior properties. Especially, the as-prepared PDES-modified superhydrophobic coating possesses an amazing chemical stability which not only can repel cool liquids but also can show excellent resistance to a series of hot liquids and hot beverages. Li and co-workers[60] demonstrated a novel method to fabricate various metal oxide (ZnO, Al$_2$O$_3$, Fe$_3$O$_4$) nanoparticles superhydrophobic coating on various substrates, such as sponge, fabric, paper, by treatment with PDMS via CVD method. The study showed that the combination of the improved surface roughness generated from of the nanoparticles aggregation with the low surface-energy of silicon-coating would be responsible for the superhydrophobicity. Our group[61] also investigated a series of VIII and IB metals and oxide nanoparticles including Fe, Co, Ni, Cu and Ag. We presented a simple and available way (Fig. 3c) to facilitate the synthesis of thiol-ligand nanocrystals superhydrophobic coating. Using iron oxide nanoparticles as a model, the main steps of fabrication showed as follows: Iron oxide nanoparticles were synthesized by a modified co-precipitation method.[62-63] Next, the clean substrates were immersed in the stored nanocrystal suspensions for about 5 minutes at room temperature. Afterwards, the substrates coated with nanocrystals were immersed inoctadecyl thiol or perfluorodecane thiol anhydrous ethanol for 24 h at room temperature. Finally, we obtained superhydrophobic/ oleophobic or superhydrophobic/ superoleophobic materials. Furthermore, the superhydrophobic and superoleophilic nanocoatings were effectively used for application in oil/water separation.
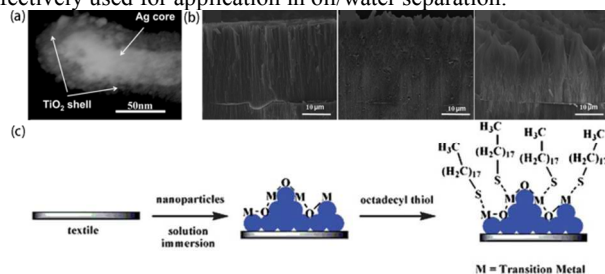
Fig. 3 (a) TEM micrograph of an isolated NR showing a silver core and a TiO$_2$ shell.[58] (b) Corresponding side-view FESEM images of the anodized alumina membranes.[59] (c) Schematic illustration of the route used to prepare thiol-ligand nanocrystals superhydrophobic coating textiles.[61] (a) Reproduced with permission from [58], Copyright (2014) Wiley-VCH Verlag GmbH & Co.

KGaA, Weinheim. (b) Reproduced with permission from [59], Copyright (2014) American Chemical Society. (c) Reproduced with permission from [61], Copyright (2012) The Royal Society of Chemistry.

Organic materials

Polymer

Polymer must be the most promising materials to construct superhydrophobic nanocoating for their flexibility, diversiform molecular design, processability and low cost. Even those most common polymer, such as polystyrene (PS), polyethylene (PE), polypropylene (PP)[64-66], can endowed with satisfying result through some simple optimization steps. For example, the water CA of PS coating could be enhanced from 95.7° to 150.6° using nanoporous AAO templates. Different geometry of surface nanostructures of PS coatings was studied and long-neck vase-like structure was recommended for optimal.[64] Low-density polyethylene (LDPE), a thermoplastic made from the monomer ethylene, is defined by a density range of 0.910~0.940 g/cm^3 and is not reactive at room temperatures. Yuan et al.[65] obtained a lotus-leaf-like superhydrophobic LDPE with CA ∼156° and low SA ∼1°. The facile fabrication steps were as follows: LDPE and NH$_4$HCO$_3$ mixture was dipped onto a cleaned glass plates. The solvents were first evaporated for 0.5 h in an atmosphere in the oven at 50 °C, and then evaporated for 2 h at 30 °C. The as-prepared LDPE coating showed excellent anti-icing property which was investigated in a climatic chamber with a working temperature of -5 °C. Pakkanen et al.[66] prepared superhydrophobic PP coating via microstructure technique and injection molding. More importantly, they demonstrated a new, novel route to protect fragile fine-scale surface topographies for improving the mechanical durability. The core idea of protection is the existence of protective sacrificial pillar with larger microscale features.

Multifarious synthetic methods are other advantage of polymer materials, such as copolymerization, atom transfer radical polymerization (ATRP), and graft polymerization process. ATRP, a kind of controllable polymerization reaction, was employed in the fabrication of surface-confined grating of glycidyl methacrylate.[67] Combined with postmodification, graft-on-graft nanocoating prepared and was used to obtain superhydrophobic bio-fiber surfaces. In particular, C$_7$F$_{15}$-functionalized graft-on-graft surface showed extremely high water CA, reaching a maximum of 172°. As illustrated in above example, fluorinated polymers are one of the most popular materials to fabricate superhydrophobic nanocoating due to their extremely low surface energy. Yuan et al.[68] synthesized a kind of fluorinated acrylic random copolymer to fabricate superhydrophobic nanocoating on Al substrate. Firstly, a fluorinated acrylic copolymer (FAC) containing hydroxyl side chains was synthesized by radical solution polymerization, then FAC was dissolved in ethyl acetate (EA) and showed aggregates of nano-scale spherical micelles. The superhydrophobic fluorinated acrylic copolymer (SFAC) coatings are simply prepared by spraying the above-mentioned micelle solution on an aluminum substrate. The obtained superhydrophobic coating not only has resistance to low temperature and excellent durability under water, exhilaratingly, but also can obviously extend water freezing time at low temperature.

Natural polymer materials are of interest as it incorporates environmentally and biologically friendly materials. Chitosan, a linear polysaccharide natural polymer, has a number of commercial and possible biomedical uses. Using chitosan-based nanoparticals, Ivanova et al.[69] developed a simple method to design the superhydrophobic anti-bacterial textile for biomedical applications. The reaction mechanism of nanoparticals fabrication was based on electrostatic interaction between amine group of chitosan and negatively charged fluoroanion which played the crucial role in the structure of aggregates in the coating and its superhydrophobicity of coatings. The researches of these special materials are relatively rare, so a wider variety of natural polymer and novel application are key points in the future.

Inorganic-organic materials

Using inorganic nanomaterials to create nanoscale or hierarchical structure on organic polymer coating is the routine thought to fabricate inorganic-organic superhydrophobic nanocoatings, which possess the advantages both of inorganic and organic materials simultaneously. Metallic oxide, Silica-based, Carbon-based the above mentioned and other inorganic materials all could be used to form organic-inorganic hybrid superhydrophobic nanocoating with polymer. ZnO/polystyrenenano composite coating was fabricated by Zhang et al.[70] via a straightforward, inexpensive method. When the ratio of ZnO nanoparticles to PS was 7:3 at temperature at 70 °C, a superhydrophobic nanocoating (WCA = 158°) can be obtained. Carbon nanotubes (CNTs) are attractive nanofillers for reinforcing polymers due to their large aspect ratio and surface area. Chakradhar and coworkers[71] prepared polyvinylidene fluoride (PVDF)–multiwalled carbon nanotubes (MWCNTs) nanocomposite coating. When the CNT content increased, a transformation from hydrophobic to superhydrophoic state has been achieved. Green method means economical, nontoxic and eco-friendly method, which was explored for the PEG-SiO_2 nanocomposite coating with superhydrophobic and transparent property by Shen et al.[72]. Molecular weight of PEG and mixed proportion of PEG/SiO_2 both have effect on wettability. According to the study, PEG 400 and 2:1 of PEG /SiO_2 were the best choices. The water CA can achieve to 168°. By spraying the suspensions of polyurethane (PU)/molybdenum disulfide (MoS_2), a wear-resistant superhydrophobic coating was obtained on various substrates.[73] The papillae-like PU/55.6%MoS_2 coating showed superhydrophobic behavior with the water contact angle of 157°. Meanwhile, after chemical modification, the coating displayed both superhydrophobicity and superoleophobicity.

Fabrications

Numerous fabrication methods have been developed for the preparation of superhydrophobic nanocoatings in the literatures, each providing varying degrees of control of the nano-micro roughness and wettability of superhydrophobic nanocoatings. For different materials, only by taking optimal method can researchers reach the ideal result. Furthermore, various methods have their own strengths and weaknesses respectively. So, the different strategies employed recently are concluded and discussed as follows.

Sol-gel process

In sol-gel process, chemical solution or sol is utilized as a precursor. When a large amount of solvent are still congested in the network during the network formation process, gel is formed after a series of hydrolysis of precursor. Because of the special process of reaction, there are few materials that meet those requirements of sol-gel process. But on the other hand, almost all kinds of solid[74-81], such as metals, silicon wafer, glass, textiles, could be as substrates to fabricating superhydrophobic coatings by sol-gel method; the other advantage to this method is controllable, for surfaces property (including surface nano-structure) depending on functional group of outcome gel and the preparing process. So, since the early stage of mimicking nature, like lotus leaves' surface, this method have been used widely. Nowadays, it still can be counted as a practical way in fabricating superhydrophobic nanocoating.

In recent paper, Jiang et al.[82] prepared the superhydrophobic ORMOSIL (organically modified silicate) double-layer double-wavelength antireflective (AR) coating through template-free sol-gel route, by silica particle surface modification using hexamethylisilazane (HMDS). This AR coating with nearly 100% transmittance at both 1064 nm and 532 nm has broad application prospect in high power laser system. Heinonen et al.[83] produced superhydrophobic functional coating with nano-sized silver particles (AgNPs) by a sol-gel coating method. First, aluminium tri-sec-butoxide ($C_{12}H_{27}AlO_3$) was used as precursor to make an alumina layer on stainless. Second, deposition of AgNPs was employed. Also a third step, the surface of coatings were modified by FAS ($CF_3(CF_2)_7CH_2CH_2Si(OCH_3)_3$) to obtain a low surface energy. Antibacterial tests showed that the surface with Ag NPs reduced the number of the bacteria. A simple sol-gel dip-coating method has been utilized by Lin[84] to prepare transparent superhydrophobic nanocoating with a sub-100 nm roughness. This nanocoating was created by using 3-aminopropyltriethoxylsilane (APTEOS) and cetyltrimethoxylsilane (CTMS) as aggregated agent and modifying agent, respectively. And this nanocoating exerted good moisture resistance. However, after heat-treating, the wettability of coating could switch from superhydrophobic (>160°) to superhydrophilic (0°) when the temperature higher than 500 °C. At the percent stage, the shortage of this way is that the sol-gel process required for a long time, about a few days or weeks, and on the other hand, the raw materials always are harmful organism.

Chemical vapor deposition

Chemical vapor deposition (CVD) has played a crucial role in superhydrophobic nanocoating preparation field for a long time. This method can be applied whether to create rough surface by building micro- and nano- particles, nanorods into ordered structures[85-92] or to depose a thin layer of hydrophobic compound on a rough surface[93-96]. Put simply, as for the preparation process in typical CVD, the wafer (substrate) is exposed to one or more volatile precursors, which react and/or decompose on the substrate surface to produce the desired deposit. On the basis of the predecessors, CVD has been developing. This fabrication method has few limitations on the type of materials that can be used.

For studying the influence of coating morphology on their static and dynamic interactions with water droplets, a series of hierarchical BN coating film with various morphologies (Fig. 4a-

b) were produced by CVD process in different growth conditions. In this study, the different wettability was attributed to surface geometrical factors. The vertically standing mikes were hydrophobic with CA of ~105°, whereas vertically standing tubes
5 formed superhydrophobic coating films with the CA reaching ~165°.[97] A successful combination of surface roughness and low surface energy is integral to a superhydrophobic silica nanoparticles coating through a novel one-step CVD and modification method.[98] Moradian et al. used
10 tetraethylorthosilicate (TEOS), vinyltrimethoxy-silane (VTMS) as the surface modifying molecule and ammonia as a catalyzer to reduce the reaction temperature. Results showed that the lowest film formation temperature is 40 °C. Guan et al.[99] described an oxidative chemical vapor deposition (oCVD) to prepared
15 transparent, superhydrophobic, and colored silicone–carbon nanocomposite coatings, the coating procedure (Fig. 4c) as follows: in an atmosphere-controlled sealed furnace, there are two electrically heating panels in this reactor. The bottom heating panel produces the decomposition temperature (T1) and the top
20 one produces the oxidative deposition temperature (T2). Both of T1 and T2 were controlled independently by thermocouples, respectively. Then, put the substrate on the support plate and the as-prepared silicone particles were scattered on the bottom heating panel. Following, the mixture gas (O_2/N_2 was ~1:4)
25 flowed into reactor and then stopped. The values of T1 and T2 were changed with a rising rate of ~30 °C·min^{-1}. This process was lasted for about 3 h. Compared with fluorine-containing reagents, this method was cheaper and environmental-friendly. A novel method reported by Zhu[60] for fabrication of
30 superhydrophobic coatings through treating various metal oxide nanoparticles, including ZnO, Al_2O_3 and Fe_3O_4, with polydimethylsiloxane (PDMS) via CVD. The characterization shows that nanoparticles aggregation with the low surface-energy of silicon-coating originated from the thermal pyrolysis of PDMS
35 would be responsible for the surface superhydrophobicity. The strong reliance on the experiment instruments and the high demand of reactive conditions has hampered the widespread use of this method.
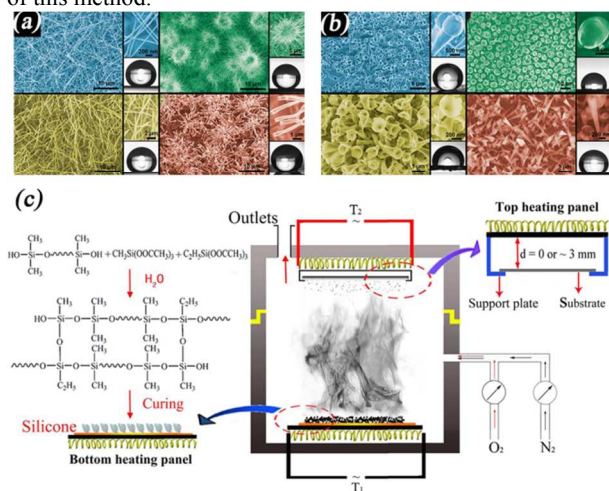
40 **Fig. 4** SEM images of BN films consisting of tubular nanostructures (a), SEM images of BN films consisting of conical nano- and microstructures (b).[97] Illustration for the experimental setup of the preparation of the colored silicone–carbon nanocomposite coatings (c).[99] (a and b) Reproduced with permission from [97], Copyright (2013) American Chemical Society. (c)

Spray process

Spray process is the most simple and practical nanocoating
50 formation method. For instance, Zhou et al.[100] prepared the emulsion solution of $[CH_3(CH_2)_{10}COO]_2Cu$ in a mixed solvent of ethanol and water first. Then the as-prepared emulsion was sprayed onto various substrates with N_2 gas and dried at room temperature. The all fabrication process was just that, well, the
55 experimental results showed that the binary micro/nanostructure superhydrophobic coating with a static water contact angle of about 160° and a sliding angle of 5° was achieved. A coralline-like structure superamphiphobic coating was fabricated[101] by spray casting nanocomposites composed of fluorinated multi-
60 walled carbon nanotubes (MWCNTs) and fluorinated polyurethane (PU). Here, superamphiphobic means that one coating surface is superhydropobic and superoleophobic simultaneously. Accordingly, this coating has wide potential application value. Large amounts of literatures related to spray
65 process had published recently.[102-103, 68] The key problems about this aspect are how to improve the adhesion force between coating and substrate and how to control the surface morphology or nanoscale roughness.

Electrospray process

70 That sounds similar to spray process and electrospray process. In fact, there are essential differences between them. Simply speaking, experimental facilities of the latter are relatively complex. The process[104] can be described generally as follows: between a syinge needle and a grounded collector, an electrical
75 potential is applied. Because of the surface tension, at the tip of the needle the solution forms a droplet slowly. When the electric voltage is sufficiently high, electrostatic repulsion between the charges that collected into the droplets can overcome the surface tension. The result is a thin jet is formed and accelerated toward
80 the collector. If the viscosity of the solutions is low enough, the solution will be sprayed in a droplet toward the collector, then forming a rough coating on substrate.

The all steps of one kind of superhydrophobic micro-nano hierarchical SiO_2 layer[105] synthesize using an electrospraying
85 process shown in Fig. 5e which is helpful for us to understand this process clearly. In the first step, Tetraethoxysilane (TEOS, $Si(OC_2H_5)_4$) and methyltriethoxysilane (MTES, $CH_3Si(OC_2H_5)_3$) were used as precursor solution of electrospraying deposition of SiO_2 layers. Then a pure SiO_2 phase was obtained. Secondly,
90 through an ultraviolet (UV)-enhanced chemical reduction process, Si nanoparticles were prepared on the surface SiO_2 layers. Namely, the micro-nano hierarchical rough surface structure was obtained. Subsequently, the dry samples were heated at 400 °C for 1h after a fluorination treatment process. The difference of
95 experimental conditions tends to bring different results, even though using the same reactants. Tang et al.[106] described a superhydrophobic coating fabrication method by electrospraying structure controlled poly(methyl methacrylate-bromine) (PMMA-Br) homopolymer and poly(methyl methacrylate)-b-poly-
100 (dodecafluoroheptyl methacrylate) (PMMA-b-PDFMA) copolymers. They found that the flow rate of the solution has

great effects on the hydrophobicity of polymer coating and at a higher flow rate, the superhydrophobic coating was obtained. Fluorinated diblock copolymers $PMMA_{50.6}$-b-$PDFMA_{0.8}$ and $PMMA_{147.9}$-b-$PDFMA_{17.5}$ superhydrophobic coatings can be obtained by electrospraying process as well at the selected flow rates, similarly. On the other hand, researchers also detected that solvent properties was closely related to the surface composition which is the major determinant of the surface wettability. During the electrospraying process in this case, THF as solvent favors C−C and C−H groups ,while DMF tend to segregation of C−O−C=O group. Therefore, the hydrophobicity will be improved with THF as solvent. X-ray photoelectron spectroscopy (XPS) detections reveal the conclusion (Fig. 5a-d). Using the elecrtospraying technique, the fabricated surfaces lack mechanical robustness for the electropraying particles easily removed from the substrate material.[107-108] Grinstaff and Yohe[109] postulated that 3D coating may be ideal for producing a generic longer-term mechanical surface. Then connected electrosprayed particle coatings were fabricated from PCL and PGC-C_{18} by this research group. By controlling the PGC-C_{18} doping concentration allow a specific superhydrophobic state to be achieved.
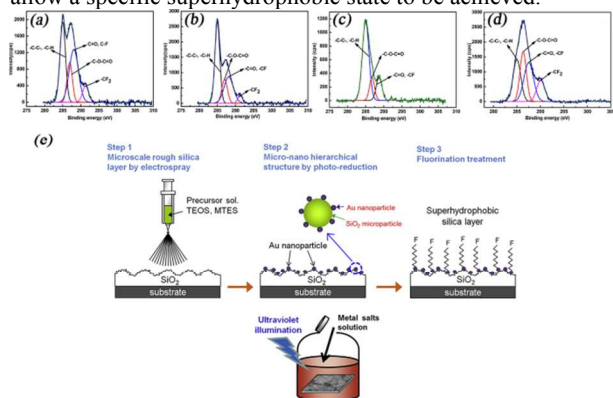
Fig. 5 C1s XPS high-resolution spectra of the $PMMA_{181.7}$-b-$PDFMA_{4.1}$ films electrosprayed from DMF (a, b) and THF (c, d) under different incident angles of 30° (a, c) and 90° (b, d).[106] (e) Illustration conceptually showing the steps used to synthesize the superhydrophobic micro-nano hierarchical SiO_2 layers in this work.[105] (a-d) Reproduced with permission from [106], Copyright (2012) American Chemical Society. (e) Reproduced with permission from [105], Copyright (2013) Elsevier.

Electrospinning process

When it comes down to micro-nano structure superhydrophobic coating fabrication process, electrospraying and electrospinning are very easy to be garbled. Strictly speaking, these two methods are similar but different. Here, the schematic diagram of electrospinning process[110] is shown in Fig. 6h to help us to understand it directly and clearly. At first, a high-voltage power is applied between a grounded collector and a feeding system which consists of a container with a liquid precursor, spinneret and a pump. The solution forms a droplet at needle tip due to surface tension. Then the electrical force elongates the droplet to a conical shape (Taylor cone)[111]. A thin jet of liquid precursor ejects from the tip of the Taylor cone when the electrical force overcome the surface tension. In the unstable electrical field, the jet begins to oscillate and move chaotically. During the chaotic motion, the jet becomes thin and solid after evaporation of the solvent. Finally, the web-like fiber coating with various micro-

nano structures is obtained on the collector. In summary, electrospinning is a promising technique for superhydrophobic coating owing to a wide set of parameters that allow effectively controlling roughness of resulted micro-nano structure fiber coating.[112-121]

Ganesh and coworkers[122] successfully used two fluorinated POSS materials (FP8 and FPSi8) (Fig. 6a) with PVDF-HFP solution to prepared superhydrophobic coating by electrospinning. The process parameters were shown as follows: The voltage applied was set to 30 kV and the distance between the static collector and the needle (27G ½) tip was 10 cm. The humidity level inside the electrospinning chamber was maintained between 50 and 60%. Precursor solutions of different wt% were electrospun on the glass substrates for 15 min with a flow rate of about 0.2 mL h^{-1}. Different wt% composite nanofiber coatings (Fig. 6b-g.) were obtained after heated at 130 °C for 4 h. As a result, with increase in the concentration of fluoroPOSS in PVDF-HFP, the water contact angle was creased for the increase of viscosity and fiber diameter thereby enhancing the superhydrophobic property. Wang et al.[123] adopted multinozzle conveyor belt electrospinning method to fabricate large-scale superhydrophobic composite coating with enhanced tensile properties through the blending of porous PS microspheres, bead-on string PVDF fibers and PAN fibers. This method can expand the electrospinning area unlimitedly and certain kinds of fibers are combined on the conveyor belt in one electrospinning step. DC-biased AC-electrospinning that induces short segments of alternating polarity can overcome electrostatic instability of the charged jet to some extent, thereby reducing the magnitude of the destabilizing force on the fiber. So, Ochanda et al.[124] fabricated Mesh-like fiber mats of polystyrene (PS) by this way. The investigation of the effect of percent weight of PS on the hydrophobicity of electrospun fiber coatings indicated that the contact angle increases monotonically with polymer weight percent and becomes superhydrophobic at 25 wt% (Fig. 6i). The reason may be that more fibers are generated with a few cases of beads-on-string morphology with an increase in polymer concentration. Some new types of electrospinning are still evolving, but one limiting factor exist which is high cost of electrospinning process. Electrospun nanocoating without any additional treatment is the focus of research in the future.
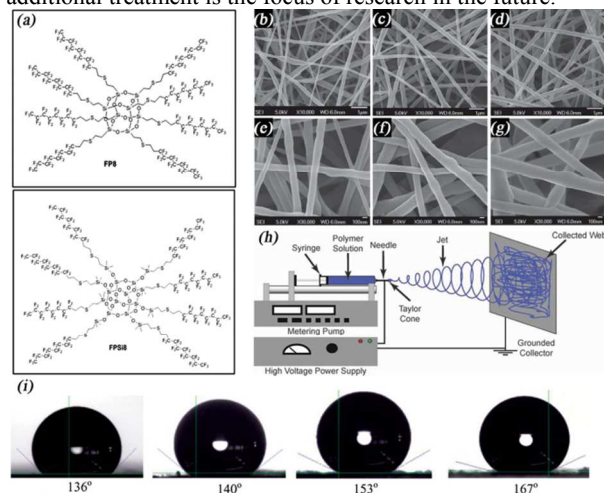
Fig. 6 (a) Molecular structures of the synthesized fluoroPOSS (FP8 and FPSi8).[122] (b and c) SEM images of PVDF-HFP nanofibers, (d and e) SEM

images of 5 wt% of FPSi8 fluoroPOSS–PVDF-HFP nanofibers, (f and g) SEM images of 15 wt% of FPSi8 fluoroPOSS–PVDF-HFP nanofibers; (h) Schematic of the basic set-up for electrospinning.[110] (i) Contact angles of fibers as a function of percent weight of polystyrene, from left to right: 15 wt%,

5 18 wt%, 25 wt%, and 30 wt%.[124] (a) Reproduced with permission from [122], Copyright (2012) The Royal Society of Chemistry. (b-h) Reproduced with permission from [110], Copyright (2012) Wiley-VCH Verlag GmbH & Co. KGaA, Weinheim. (i) Reproduced with permission from [124], Copyright (2012) Wiley-VCH Verlag GmbH & Co. KGaA, Weinheim.

10

Electrodeposition

Due to the intensive demand in the elaboration of superhydrophobic nanocoating through low-cost, reproducible and fast methods, the use of strategies based on electrodeposition

15 (Electrochemical deposition) have exponentially grown these last few years. One of the main advantages of the electrochemical processes is the relative easiness to produce various surface morphologies and a precise control of the structures at a micro- or a nanoscale.[125-130,136] In short, electrodeposition can be divided

20 into two categories according to the different kind of deposit that will be elaborated in the following sections.

Electrodeposition of metal represents a suitable method to fabricate superhydrophobic coating. Electrodeposited Ni surfaces exhibited superhydrophobic properties strongly depending on the

25 morphology of the coating. Hierarchical flowerlike structures Ni-Co alley coating with a WCA as high as $167.3 \pm 1.3°$ and an ultra-low sliding angle of about 1° prepared on AZ91D magnesium alloy was reported by Li et al.[131] through electrodeposition after modified by stearic acid. According to Fig.

30 7, they found the modification process changed surface morphology not too much but changed CA a lot. Especially important, this Ni-Co alley coating has good chemical stability and long-term durability as well as the self-cleaning effect, highly anticorrosion ability. Similarly, We et al.[132] reported a

35 superhydrophobic Ni-Cu-P alloy coatings with high mechanical strength by one-step galvanostatically electrodeposited onto low alloy steel substrates. However, the difference is this kind of coating has strong adhesion force (Fig. 8a) and the mechanism of the high adhesion characteristic was explained by Cassie

40 impregnating model (Fig. 8b.). Co-based superhydrophobic powder coating also was obtained[133] n electro-deposition process as follows: cobalt chloride (0.056M) and myristic acid (0.1 M) were added into the ethanol under stirring until a uniform electrolyte solution (150 ml) was obtained. Then two cleaned

45 stainless steel plates were taken as the cathode and anode in an electrolyte cell. After electrolysis time of several minutes, as-prepared cathodic surface was obtained. Cu superhydrophobic coating with nano-structure was prepared by Li and coworkers[134] like the above metal. But magnesium alloy cannot be used as

50 substrates for the high reactive nature. So, in this paper, Ni electroless plating was used as pre-treatment method. The coating was electrodeposited under direct current conditions after Ni electroless plating. At last, the most important step is that Mg alloy with Cu coating had to be modified in an ethanolic lauric

55 acid solution which contained sodium acetate to enhance electrical conductivity. The modification process shown in Fig 8c, a reaction between the Cu_2^+ and the lauric acid electrolyte results in the formation of copper laurate, which deposits on the copper coating and disperses in the solution. At the same time, the

60 surface could absorb some lauric acid by electrostatic interaction.

The modification decreased the surface energy of Cu coating rapidly.

Electrochemical deposition of substituted organic conducting polymers allows generating superhydrophobic structured coating

65 on conductive substrates. This method always means a one-step process to make rough low-energy surfaces while no hydrophobization post-treatments are required. For example, a fluorinated monomer (EDOT-F8) is used to reach superhydrophobic properties via electrodeposition process by

70 Guittard et al..[135] Their group also[137] synthesized an original fluorinated EDOT derivative by grafting an F-octyl tail directly onto an EDOT heterocycle and was used to fabricate superhydrophobic nanocoatings by electrodeposition. Interestingly, the surface was composed of nanofiber arrays at

75 low deposition charges (between 100 and 200 mC·cm^{-2}) with low hysteresis. However, the nanofibers formed flower-like structures sticky coating at high deposition charges (above 200 mC·cm^{-2}).

In general, due to the intensive demand in the fabrication of superhydrophobic nanocoatings using reproducible, low-cost,

80 mild-condition and fast methods, electrochemical processes have exponentially grown these last few years. But without ignorance, electrochemical processes unable to precisely control the nanoscale roughness and have certain randomness.
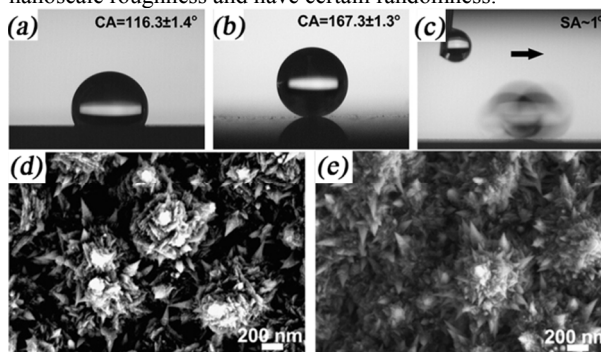
85 **Fig. 7** (a) CA image of the electrodeposited Ni–Co alloy coating; (b) CA and (c) SA images of the as-prepared hierarchical flowerlike structures superhydrophobic surface. SEM images of the electrodeposited Ni-Co alloy coating (d) and the as-prepared hierarchical flowerlike structures superhydrophobic surface (e).[131] Reproduced with permission from [131],

90 Copyright (2014) Elsevier.
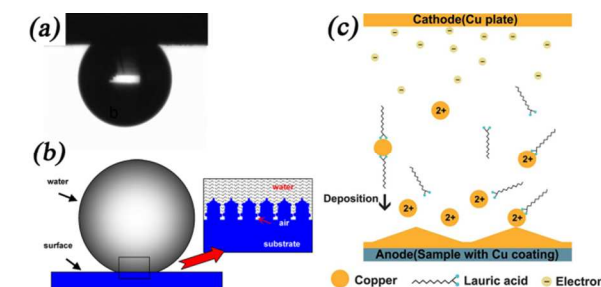
Fig. 8 (a) Optical graphs of a water droplet on the as-deposits alloy coating; (b) Schematic illustration of the Cassie impregnating wetting state.[132] (c) The

95 schematic diagram of the modification process of Mg alloy with Cu coating in an ethanolic lauric acid solution.[134] (a and b) Reproduced with permission from [132], Copyright (2013) Elsevier. (c) Reproduced with permission from [134], Copyright (2012) The Royal Society of Chemistry.

Hydrothermal method

100 Hydrothermal synthesis, also termed "hydrothermal method",

includes the various techniques of crystallizing substances from high-temperature aqueous solutions at high vapor pressure. This method can be used to create crystalline phases which are unstable at the melting point and materials which have a high vapour pressure near their melting points can also be grown by the hydrothermal method. Based on the above advantages, this method has been applied to fabricate superhydrophobic nanocoating to control the surface crystal morphology preferably for a long time.

Wang et al.[138] has reported a hierarchical structure fibrous szaibelyite synthetic method by a facile hydrothermal process: 0.025 mol $Mg(NO_3)_2 \cdot 6H_2O$ and 0.05 mol H_3BO_3 were dissolved in 100 ml deionized water, and the pH value of the solution adjusted to 7–8 by adding $NH_3 \cdot H_2O$ (25%) to the solution dropwise. Then, the as-prepared solution was transferred into a Teflon-lined stainless steel autoclave liner. The clean Mg alloy plate was immersed into the solution. The autoclave was then heated at 180 °C for 5 h. When the reaction system was cooled down to room temperature naturally, the szaibelyite film was obtained. Finally, after modification with fluoroalkylsilane (FAS), the films exhibited advantageous superhydrophobic properties with a static water contact angle of 166° and a sliding angle less than 5°. SEM images showed the morphologies $MgBO_2(OH)$ changed with different reaction times (Fig. 9a-h). After treatment for over 5 h, szaibelyite crystals grow up and self-assemble together to form spherical-like structures on the surface of the Mg alloy. The main chemical reactions are as follows:

$$Mg + 2H_2O \rightarrow Mg^{2+} + 2OH^- + H_2 \tag{1}$$

$$H_3BO_3 + OH^- \rightarrow B(OH)_4^- \tag{2}$$

$$B(OH)_4^- + Mg^{2+} + OH^- \rightarrow MgBO_2(OH) + 2H_2O \tag{3}$$
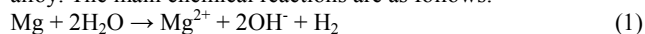
Additionally, the film still maintained substantial corrosion resistance performance after immersion in 3.5 wt. % NaCl solution for 32 days.

Under modified hydrothermal (MHT)[139] conditions at 100 °C, a simple, cost effective way to deposit nanocolumnar ZnO coating which brought out UV switchable reversible wettability shown on Fig. 9i on glass slides has been observed by pal et al.[140] The researchers explained the mechanism of this transition as follows: Due to UV light illumination an electron–hole pair is generated in the ZnO thin film. Some of the holes react with lattice oxygen leading to oxygen vacancies in the film. The photogenerated electrons are captured by lattice Zn^{2+} to form Zn_s^+, surface trapped electron sites. Zn_s^+ and surface trapped water molecules react with each other and form Zn_s^{2+}. Very similar to last example, another kind of stearic acids-modified Fe_2O_3 nanorod coating with tunable water adhesion was prepared via hydrothermal procedure at 120 °C.[141] The crystal growth time of the precursor would be the determining factor to superhydrophobicity and water adhesion. Up to now, many similar great papers[142-146] has been published, but how to apply this method to industrial production may be a current issue.
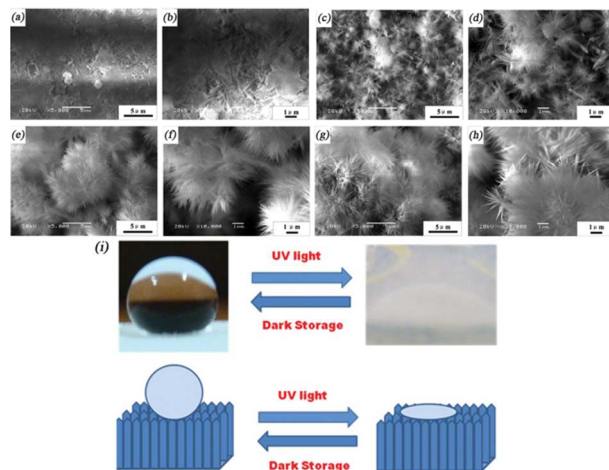
Fig. 9 SEM images of sample surfaces after hydrothermal treatment at 180 °C for (a) 2 h, (c) 4 h, and (e) 5 h, (g) 6 h; (b), (d), (f), and (h) are the enlarged SEM images of (a), (c), (e), and (g), respectively.[141] (i) UV switchable reversible wettability of ZnO with a nanocolumnar morphology.[142] (a-h) Reproduced with permission from [141], Copyright (2014) Elsevier. (i) Reproduced with permission from [142], Copyright (2010) Wiley-VCH Verlag GmbH & Co. KGaA, Weinheim.

Solution immersion process

Solution immersion process is a simple and universal one-step process to render substrates superhydrophobic by immersion the substrates in a solution that generally contains low-surface-energy agents. However, the defects of this method are unstable for coatings and time-consuming. Control of the nano-roughness is difficult by this way as well. For the coexistence of advantage and disadvantage above-mentioned, many researchers still attempt to make progress in this aspect.

One of recently reported example was based on the use of pristine multiwall carbon nanotubes (MWNTs) and polybenzoxazine in a solution immersion process to construct nanocomposites coating on ramie fabric by Yan et al.[147] A complete cycle is as follows: first, the ramie fabric was immersed into the MWNTs/benzoxazine monomer (3,3'-(((2,2-dimethylpropane-1,3-diyl)bis(oxy))bis(4,1-phenylene))bis(3,4-dihydro-2H-benzo[e][1,3]oxazine-6-carbonitrile), BOZ) mixture suspension, then washed several times with deionized water and ethanol, dried under vacuum, at last heated at 130 °C. The WCA value of MWNTs/BOZ mixture suspension (MWNTs: 1.0 mg mL^{-1}, BOZ: 1.0 mg mL^{-1}) for 20 cycles can reach 152°. Finally, the relationship of superhydrophobicity and conductivity with the number of repeated cycles and the concentration of MWNTs suspension is highlighted. Clean commercially obtained copper foam was used as substrates to prepare non-flaking superhydrophobic coating by Xu et al.[148] through one-step solution-immersion process. Copper stearate with micro- and nano-scale hierarchical surface morphology (Fig. 10b) can be obtained after copper foams immersed in ethanolic stearic acid solution for several days at room temperature. The reaction can be expressed as follows:

$$2Cu + O_2 + 4H^+ \rightarrow 2Cu^{2+} + 2H_2O \tag{1}$$

$$Cu^{2+} + 2CH_3(CH_2)_{16}COOH \rightarrow Cu[CH_3(CH_2)_{16}COO]_2 + 2H^+ \tag{2}$$
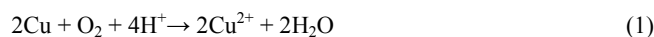
Through the oxidation of copper, Cu^+ ions are released from the

substrates and react with stearic acid immediately to form copper stearte. Further study revealed that this superhydrophobic coating on copper foam are much more roust with better mechanical stability then flat copper plate. Wang et al.[149] prepared a series of superhydrophobic light alloys (including AZ91D Mg alloy, 5083Al alloy, and TC4 Ti alloy) by immersing the substrates in 1H,1H,2H,2H-perfluorooctyltrichlorosilane (PFOTS), ethanol, and H_2O/H_2O_2 mixed solution (Fig. 10a). Through this one-step method, the light alloys are in possession of micro/nano surface structures and low surface-energy at the same time.

Composite techniques

Composite technique is a practical method to tune the surface morphology of nanocoating to create the superhydrophobicity. Lee et al.[150] used a hybrid method, a combination of nanoimprint lithography and hydrothermal growth, to fabricated ten kinds of TiO_2 structures. Nanoimprint lithography was used to create a microstructure and hydrothermal growth was to create nanostructure. This also is a routine thought of other composite techniques. As a result, TiO_2 hierarchical structures formed the most stable superhydrophobic state and the longest time for natural evaporation of water as well. Ding et al.[151] prepared F-PBZ/SiO_2 NP (fluorinated polybenzoxazine/SiO_2 nanoparticle) modified SNF (silica nanofibers) membranes through the combination of electrospinning process and in situ polymerization. At first, SNF was fabricated by electrospinning process with an applied voltage of 18 kV and a controllable feed rate of 1 mL h^{-1}. Then F-PBZ/SiO_2 NP modification was accomplished by dipping the membranes in the solutions of different concentrations of BAF-tfa with various concentrations of SiO_2 NPs. Then in situ polymerization of BAF-tfa was carried out at 190 °C in a vacuum for 1 h, which was the second step (Fig. 10c). The resultant coating have maintained the super water-repellency even after the heat treatment of 450 °C. Couda and coworkers[152] obtained two kinds ZnO seed layers by a physical vapor deposition approach and a wet-chemical route, namely, the radio frequency magnetron sputtering and the spin-coating techniques, respectively. Through a hydrothermal method, ZnO nanowires (NWs) were grown on each kind of seed layer. A time-dependent behavior of the wetting properties was found for both sputtered and spin-coated seed layers. Fresh or aged NWs grown on the sputtered seed layer showed superhydrophobic behavior (WCA ca. 180°). However, the NWs grown on spin-coated seed layers are quite hydrophilic (average WCA ca. 40°). The reason can be illustrated by IR spectroscopy for a hydroxyl-rich surface of the NWs from spin-coated layers. In contrast, a lower amount of -OH groups existed on NWs grown on the sputtered seed layers. Template method and chemical vapor deposition CVD process was employed in the fabrication of nano- and micrometer scales superamphiphobic coating.[153] A glass slide was held above the flame of a paraffin candle, then deposition of a soot layer which was consisted of carbon particles with a typical diameter of 30-40 nm. Making use of CVD of tetraethoxysilane (TES) catalyzed by ammonia, researchers coated the soot layer with a silica shell. To remove the carbon core and a decrease in the shell thickness, calcinating the hybrid carbon/silica network at 600 °C for 2 hours in air was a good way. After semi-fluorinated process, a water/organic liquid drop placed on top of the coating formed a

static contact angle > 150°, with a roll-off angle < 5°. Additionally, the coating keeps its superamphiphobicity after being annealed at 400 °C. Namely, this superamphiphobic coating can survive harsh conditions.
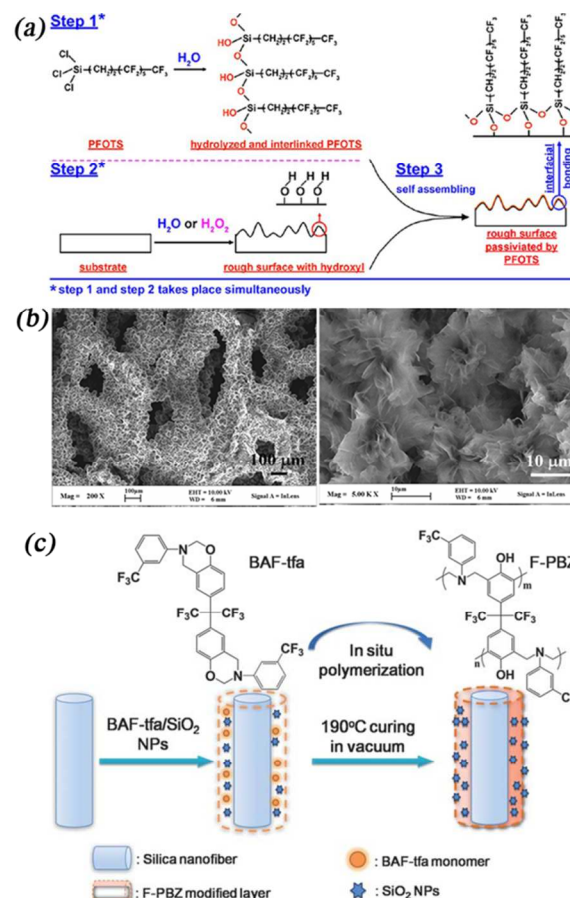
Fig. 10 (a) Possible covalent bonding mechanism of PFOTS to the substrate.[140] (b) FE-SEM images of copper foams prepared via the one-step solution-immersion process with immersion times of 4 days, and higher-magnification versions (right).[139] (c) Illustration showing the synthesis procedure of F-PBZ/SiO_2 NP modified silica nanofibrous membranes and the relevant formation mechanism.[151] (a) Reproduced with permission from [140], Copyright (2013) American Chemical Society. (b) Reproduced with permission from [139], Copyright (2014) Elsevier. (c) Reproduced with permission from [151], Copyright (2012) The Royal Society of Chemistry.

Others techniques

Besides of the methods referred above, the application of some new methods in fabrication of superhydrophobic nanocoating has got more and more attention in recent few years.[154-158] Egorkin et al.[159] described a method of preparation and electrochemical properties of superhydrophobic nanocomposite coatings on the surface of magnesium alloy pretreated using plasma electrolytic oxidation (PEO). For this coating, the values of the contact and rolling angles are 166° ± 3° and 5° ± 3°, respectively. Large-scale superhydrophobic PU/nano-Al_2O_3-Al coatings were successfully fabricated by a suspension flame spraying process to further enhance the anti-corrosion performances of Al coatings.[160] And this coating showed tunable superhydrophilicity/superhydrophobicity as achieved by changing

the concentration of PU in the starting suspension. Kitagawa and coworkers[161] demonstrated a new way to superhydrophobic porous coordination polymers by incorporating an anisotropic crystal morphology featuring a predominant surface without any need for postsynthetic modifications. What is more, bulk water is repelled as a result of the exterior surface corrugation but hydrophobic organic molecules and water vapor are able to penetrate the surface and be densely accommodated within the pores. Teiasla et al.[162] introduced a new thermal spray method called the Liquid Flame Spray (LFS) for generating nanoscale coatings in a continuous roll-to-roll process at normal pressure. The highest measured water contact angles on the nanocoated paperboard surface were over 160° and falling water droplets were able to bounce off the surface. Affordability and continuous nature of the process are the biggest benefits of LFS nanoscale coating.

Applications

The application of superhydrophobic nanocoatings is the destination and purport of all researches; every theory, materials and fabrications all serve these fundamental goals. A number of principles have demonstrated for many applications, such as oil–water separation, corrosion resistance, self-cleaning and so on, which remain a major concern as well as in this review though it still have a long way to go before them can be used in daily life. For the purpose of facilitating the comparison of various fabrication methods and materials in relation to the different applications, some references information has been summarized in Table 2 clearly.

Oil–water separation

In the last few years, the frequently occurring leakage of organic pollutants into water and industrial oily wastewater continuously threatens ecological system.[163] Therefore, separation of water and oil mixture has been considered as key challenge. Actually, many available methods based on common adsorptive has been developed for oil cleanup, such as zeolites, activated carbon, natural clays, straw, and wool fibers.[164] However, the currently materials always suffer from hydrophilic nature, leading to a poor selectivity for organic pollutants. To solve this problem, special wettability materials have been developed over the past decade. Based on different surface wettability, materials applied in this field can be organized into three types: "oil-removing" type, "water-removing" type and smart controllable separations type.[163] Here, we will mainly discuss "oil-removing" type. "oil-removing" type can filter or absorb oil from oil/water mixture selectively for their unique superhydrophobic and superoleophilic. Considering the distinct difference in surface tension between water (72.8 mN m^{-1}) and oil (<30 mN m^{-1}), superhydrophobic surfaces which are commonly oleophilic or superoleophilic[13], which also is the fundamental reason why oil can be separated from water. Furthermore, the "oil-removing" type can be divided into two categories as well: oil filtration materials and oil absorbent materials.

Superhydrophobic meshes are the main representative for the first category. For instance, Feng et al.[165] reported micro- and nano- structures TiO$_2$ coated mesh which could be used for the separation of insoluble oil from water (Fig. 11a) due to its special wettability. Copper mesh coated with extremely rough silicone elastomer was found to be exceptionally efficient in separating organic solvents (hexane, petroleum ether and toluene) from water by Parkin et al.[166] For example, the water can bounce on the surface and the toluene sinks in and spreads outward shown in Fig. 11b.

Absorbent materials, the second category, can concentrate oil into a semisolid phase and transform oils by removal of the absorbent materials. High selectivity, good recyclability, graphene-based sponges (Fig. 11c) was prepared by Tai and coworkers.[167] Excellent absorption capacities of this sponge can up to 165 times their own weight. This result showed promise for large-scale application. The adhesion between substrates and nanocoating is always poor, which is main challenge in study. Pan et al.[168] fabricated a robust superhydrophobic 3D porous material through a one-step solution immersion method which exhibited high oil absorption capacity and high selectivity shown in Fig. 11d. The superhydrophobic sponges could be reused for oil–water separation for more than 300 cycles without losing their superhydrophobicity. As a matter of fact, the investigations in this field are still facing a lot of challenges, and some of the problems still need to be solved. Foremost, most of the surface micro- and nano- structure can be easily destroyed by mechanical stress and chemical contamination. And most of the previous works have focused on low-viscous oil and water mixture but few on the separation of high-viscous oil-and-water mixtures.[163]

Fig. 11 (a) Image of the experimental process of water purification using a doublelayer TiO$_2$-based mesh film: Left, methylene blue aqueous solution and petroleum ether stay on the mesh film before separation; Right, only the aqueous solution stays after the separation.[165] (b) Photograph showing the interaction of superhydrophobic mesh (pore size – 152 mm) with toluene and water.[166] (c) Snapshots of the removal process of motor oil (dyed with Solvent Red 24 for clear observation).[167] (d) Oil-absorption capacities of the superhydrophobic sponges for oils and nonpolar solvents.[168] (a) Reproduced with permission from [165], Copyright (2013) The Royal Society of Chemistry. (b) Reproduced with permission from [166], Copyright (2013) The Royal Society of Chemistry. (c) Reproduced with permission from [167], Copyright (2012) The Royal Society of Chemistry. (d) Reproduced with permission from [168], Copyright (2013) The Royal Society of Chemistry.

Corrosion resistance

"Corrosion" is the term used describes the destruction of a metal by chemical or electrochemical reactions between the metal and its environment.[169] Corrosion reaction creates enormous waste of metal resources every year. Traditional anti-corrosive methods including oil paint and treatment with chromium containing compounds are harmful to human health and environmental which have significantly limited their broad applications.[170] During the past two decades, researchers have found superhydrophobic nanocoating without heavy-metal composite can be listed as a much more effective method to cover

various material surfaces to prevent this from corrosion.[171-177] This method have attracted much attention both from basic research and technological applications, and the corrosion resistance mechanism of superhydrophobic surface coating is
5 mostly contributed by the existence of air pockets between the substrate and solution, providing an effective blocking to fight against the migration of corrosive ions (e.g. chloride ions in seawater).[178]

Advincula et al.[179] managed to fabricate the dual properties
10 superhydrophobic anticorrosion nanostructured conducting polymer coating by a two-step coating procedure which can be used to coat any metallic surface. The corrosion resistance of this nanocoating was investigated by using potentiodynamic polarization scans in chloride solution of different pH and
15 temperature for up to 7 days. The results showed that protection efficiency of this coating was greater than 95%. Xiong et al.[180] generated a series of superhydrophobic membranes (Fig. 12a) with different surface morphologies and chemical compositions by sol-gel method. The humid air test demonstrated that the
20 potentiodynamic polarization curve and superhydrophobicity were not adequate to assess the anti-corrosion ability; the tendency occurrence of electrolyte film should be taken into consideration. Furthermore, the surface morphology played more important role than the surface chemical composition in anti-
25 corrosion ability. In order to study the anti-corrosion properties of the coatings on the Mg-Mn-Ce alloy, three types of coating with different wettability from hydrophilic to superhydrophobic in 3% aqueous solution of sodium chloride were s corrosion selected.[181] It have known that corrosion potential is a measure of tendency
30 of the sample to corrode, as higher corrosion potential indicates better corrosion resistance.[182] Superhydrophobic nanocomposite coating formed on the magnesium alloy by a PEO process has the best corrosion properties according to potentiodynamic polarization curves (Fig. 12c). The small fraction of the wetted
35 area and weak bound between hydrophobic agent molecules with coating material contributed to this result together. Li et al.[160] successfully fabricated large-scale corrosion-resistant superhydrophobic PU/nano-Al$_2$O$_3$-Al nanocoatings. The layer containing 2.0 wt% PU displayed excellent superhydrophobicity
40 with the contact angle of ∼151°and the sliding angle of ∼6.5° for water droplets. The potentiodynamic polarization testing (Fig. 12b) showed the corrosion potentials of the Al coating and the PU/Al$_2$O$_3$coating are −1.357 V and −1.207 V, respectively. The positive shift in corrosion potential suggests the efficient
45 protection by the superhydrophobic coating.
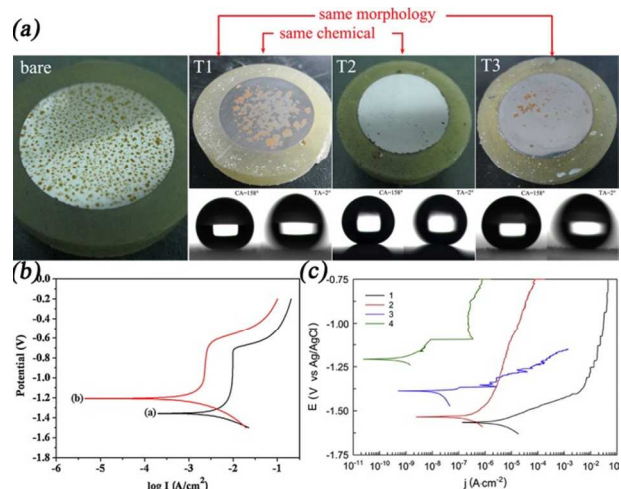
Fig. 12 (a) Photos of different samples and the wettability of prepared membranes after humidity test.[180] (b) Potentiodynamic polarization curves of (black) the superhydrophilic Al coating and (red) the superhydrophobic
50 PU/Al$_2$O$_3$/Al coating measured in 3.5 wt.% NaCl aqueous solution.[160] (c) Potentiodynamic polarization curves in 3% NaCl for the investigated samples: uncoated MA8 alloy—1; PEO coating—2; hydrophobic coating—3; and superhydrophobic nanocomposite coatings—4.[181] (a) Reproduced with permission from [180], Copyright (2014) Elsevier. (b) Reproduced with
55 permission from [160], Copyright (2014) Elsevier. (c) Reproduced with permission from [181], Copyright (2011) Elsevier.

Self-cleaning property

Lotus leaves can always keep a clean appearance despite in a mire environment in nature.[9, 19, 21] Studies had found that the
60 cooperation between hierarchical structure and epicuticular wax on the leaves surface contributed to a high CA and a low SA. So water droplets can roll off instead of sliding on the surface and take away the dirt adhered on its surface effectively. This promising property is called the "self-cleaning".[6, 19, 183-187] Up to
65 now, many artificial self-cleaning superhydrophobic nanocoating have been synthesize by different method and been applied in diverse domains industry, daily life, and military.[188-193]

Lyons et al.[194] fabricated multifunctional TiO$_2$−high-density polyethylene (HDPE) nanocomposite coatings exhibiting
70 superhydrophobicity and self-cleaning properties by using mesh template and embedding untreated TiO$_2$ nanoparticles. Self-cleaning properties tests showed the water droplets could clean away course alumina sand and fine graphite powder on the superhydrophobic coating surface (Fig. 13a-c). However, on
75 smooth HDPE surface water droplets adhered to the surface and lose the self-cleaning properties (Fig. 13d). Rodriguez et al.[195] also obtained two types lotus-like hierarchical superhydrophobic coating surface by assembled templates and nanoimprint method with sliding angle from 4° to 7°. The self-cleaning property of
80 this superhydrophobic surface was extremely similar to lotus leaf. But, why rolling droplets can take away the dirt, even hydrophobic one, adhered on superhydrophobic surface? Energy degrades would be the first reason. When a spherical particle (dirt) attaches to a liquid interface (Fig. 13e), the area of the sphere that
85 becomes wetted can be described by Eq. (8) and liquid also loses some interface, given by Eq. (9) (R$_s$ being the radius of the sphere).

$$2\pi R_s^2(1 + \cos\theta_e) \qquad (8)$$

$$\pi R_s^2 \sin^2 \theta_e \qquad (9)$$

The change in surface energy can be calculated as:

$$\Delta F = 2\pi R_s^2 (1 + \cos \theta_e)(\gamma_{SL} - \gamma_{SV}) - \pi R_s^2 \sin^2 \theta_e \, \gamma_{LV} \qquad (10)$$

Substituting with Eq. (1) gives

$$\Delta F = -\gamma_{LV} 2\pi R_s^2 (1 + \cos \theta_e)^2 \qquad (11)$$

when the equilibrium contact angle (θ_e) is not 180° or 0° for a particle moving into the liquid, it is always tend to attach a sphere. A second reason in the removal of dirt from a roughened surface is the reduction in solid/solid interfacial area for the particles sit on top of small-scale roughness without strongly constraint. Impacting drops can enter the larger scale of roughness and collect particles from the crevices of the larger scale roughness, which is the last reason of dirt removal.[196]

Chen et al.[197] demonstrated a unique self-cleaning mechanism using the cicada wing as a model surface (Fig. 13f): contaminants are autonomously removed by the self-propelled jumping motion of the resulting liquid condensate. The power of jumping motion off the superhydrophobic surface comes from the surface energy released upon coalescence of the condensed water phase around the contaminants. This finding would offer insights for the development of new self-cleaning coating.
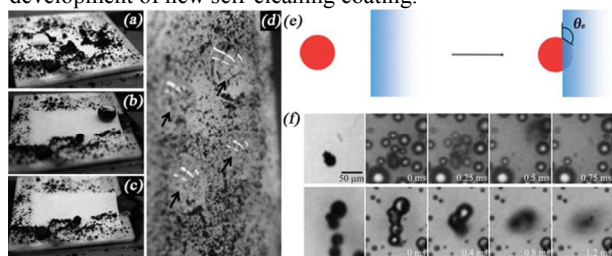
Fig. 13 (a-c) Self-cleaning effect of water droplets on the TiO2-HDPE composite superhydrophobic surface, and (d) sticky water droplets (marked) on a normal flat HDPE surface put vertically. (The black contaminates are fine carbon particulates with an average size of 1 μm).[194] (e) A hydrophobic, spherical particle moving from the air to a position in water interface where it has its contact angle with the liquid.[196] (f) Self-cleaning by the jumping condensate on horizontally held cicada wings. (Up) Removal of a single pollen particle after coalescence with neighboring drops. (Down) Removal of multiple silica particles upon coalescence.[197] (a-d) Reproduced with permission from [194], Copyright (2013) American Chemical Society. (e) Reproduced with permission from [196], Copyright (2013) John Wiley & Sons, Ltd. (f) Reproduced with permission from [197], Copyright (2013) PNAS.

Anti-icing

Each year, the ice storm causes billions of dollars in damage to the power networks, telecommunication equipment, highway, and other public infrastructures.[198] Under these circumstances, various anti-icing and deicing methods have been developed.[199] However, conventional methods (e.g. freezing point depressants, electrothermal method, and mechanical method) both require considerable energy and economical cost.

Within the past few years, bio-inspired superhydrophobic nanocoating has been proposed to be used in this field.[200-203] For air trapped inside surface textures, superhydrophobic nanocoating has small contact angle hysteresis, so the water droplet slides easily before freezing.[204, 205] As to impacting water droplets, superhydrophobic nanocoating has been proposed to prevent accumulation, as droplets can bounce the superhydrophobic surface before ice nucleation takes place even in supercooled conditions.[206] Chen et al.[207] prepared four aluminum surfaces from superhydrophilic to superhydrophobic by combining an etching and a coating process. Water droplet impact dynamic study showed that single and successive water droplets could rebound on the superhydrophobic surface and roll off at a tilt angle larger than 30° under an extremely condensing weather condition. Namely, the superhydrophobic surface had a strong icephobic property. By spraying a fluorinated acrylic random copolymer micelle solution, a superhydrophobic nanocoating was obtained.[68] And this coating displayed anti-icing properties. Fig. 14a showed that the water droplet on the hydrophobic hydrophobic fluorinated acrylic copolymer coating rapidly began to freeze after 5 seconds (delay time) and freezed completely after 29 s. A longer delay time (about 43 s) was required for the droplet on the superhydrophobic hydrophobic fluorinated acrylic copolymer coating to initiate freezing, and the end of freezing was at about 80 s. superhydrophobic multi-walled carbon nanotubes (MWNT)–silicone composite films fabricated by Han et al..[54] Anti-icing performance study (Fig. 14b) showed the growth rate of the frost on the superhydrophobic coating was about a half of that on the bare Al surface. A simple and low-cost technique was employed in the fabrication of silicon-oil-infused polydimethylsiloxane (PDMS) nanocoatings.[208] This coating was designed for icephobic application and its ice-phobic property has been investigated. As a result, this coating surface showed a low surface energy and low ice adhesion strength (Fig. 14c), only about 3% of the value on a bare aluminum surface.

The relationship between superhydrophobicity and icephobicity of s surface is currently under debate. Some researcher claimed that superhydrophobicity and icephobicity of surface are parallel rather than directly.[209] The absence of a standard to characterize ice adhesion strengths, the difference of preparation of ice samples and tasting procedure all may be a reason.[199] The process of icing upon superhydrophobic surface is quite complex. Although, recently research has leaded to a better understanding of icing phenomenon, the basic research of freezing mechanism, ice nucleation and growth and ice adhesion strengths are still necessary to study in the future.
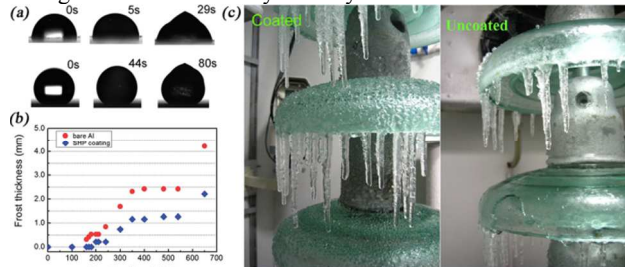
Fig. 14 (a) Photographs of the profiles of individual water droplets on HFAC (up) and SFAC coating (down) during the whole freezing process captured by a high speed CCD camera.[68] (b) Comparison of frost growth rate on the superhydrophobic (SHP) coating (20 vol% MWNT) with that on a bare Al substrate.[54] (c) Ice formed on PDMS coated and uncoated surface of an insulator under a condensing weather condition at −5 °C and saturated humidity.[208] (a) Reproduced with permission from [68], Copyright (2013) The Royal Society of Chemistry. (b) Reproduced with permission from [54],

Drag-reducing

Drag phenomena is one of the main hindrances for shipping, microfluidic devices and submarines for the friction between water/solid interfaces. In nature, there are many materials that own special drag reduction ability.[210] Two kinds of surfaces had been developed learning from natural wisdom: rib-structured surface inspired by shark skin[211], or superhydrophobic surface inspired by lotus leaf.[212] Here, we mainly focus on the latter one, superhydrophobic surface would form a thin layer of air which decrease the water/solid contact area then achieve the dray reduction effect.[213]

Since the dray-reduced phenomena for superhydrophobic coating surface in 1991[214], this research filed has been investigated both theoretically and experimentally. It terms recent research; there are a number of successful examples: Moaven et al.[215] has investigated the drag reduction of superhydrophobic nanocoating in laminar and turbulent flows. Comparing the frictional drag force on an aluminum disc with TiO_2 superhydrophobic nanocoating and a smooth coatless aluminum disc, results indicated the drag reduction values of up to 30% and 15% in laminar and turbulent flows, respectively. Chen et al.[216] obtained a normal ball with a superhydrophobic coating via dip-coating process. The superhydrophobic ball and normal ball rolled separately down an L-shaped steel channel and then floated horizontally on the water surface (Fig. 15a-e). The average velocities of the movement of the two balls calculated to be 27.0 cm min^{-1} for the superhydrophobic ball and 12.5 cm min^{-1} for the normal ball. That is to say, the superhydrophobic coating can reduce the fluid fraction dray observably. However, Wei and coworkers[217] putted forwards a new perspective that the dray-reducing effect of superhydrophobic coating was mainly cause by plastron effect instead of the decrease in the wetting area. They fabricated a superhydrophobic coating by electroless deposition of gold aggregates. And this superhydrophobic model ship exhibited a remarkable drag reduction of 38.5% at a velocity of 0.46 m s^{-1}. Furthermore, a decrease in the wetting area for the superhydrophobic object does exist but only 5.8% difference between both, which has little impact on the final drag reducing effect. So, plastron effect was thought to be the primary cause according to slip boundary[218-220] theories and the hypothesis in Newton's law of viscosity. More specifically, with a plastron, the drag force on the superhydrophobic model ship was mainly caused by liquid/bubble/solid friction, which was less than the liquid/solid friction on the normal ship.

Anti-bacteria

Anti-bacteria are of concern in numerous applications ranging from biosensors to biomedical implants and devices, and from food packaging to industrial and marine equipment.[221, 222] For example, microbial proliferation on an implant is responsible for many hospital-acquired infections that occur annually.[223] In order to address this problem, it is highly desirable to design coatings that reduce bacterial adhesion passively or release antimicrobial agents.[224] For example, Schoenfish et al.[225] prepared superhydrophobic nitric oxide (NO) - releasing xerogels by a spray process. The combination of superhydrophobicity and NO release would result in even greater antibacterial performance than either strategy alone. The killing effect of NO was demonstrated at longer bacterial contact times, with superhydrophobic NO-releasing xerogels resulting in 3.8-log reductions in adhered viable bacteria vs. controls. Ivonova and Philipchenko[69] developed a simple method to design superhydropobic anti-bacteria chitosan-based coatings. This anti-bacterial functionality of coating is supported by using chitosan-based nanoparticles.

Silver nanoparticles on the superhydrophobic framework always have a great effect of anti-bacteria based on the release of silver cations (Ag^+). It has been suggested that upon the penetration of Ag^+ ions into the bacterial cell, the DNA molecule loses its replicability, eventually leading to cell death[29], though the antimicrobial mechanism of Ag^+ ions is not yet fully understood. Superhydrophobic silver-containing coating was prepared using a sol-gel technique by Heinonen et al.[83]. Silver nanoparticles were reduced on the surface of the prepared γ-alumina layer by Tollens process then the composite coating was modified by FAS to obtain a low surface energy. The anti-bacteria activity of uncoated steel, coated superhydrophobic steel and coated superhydrophobic silver-containing steel were introduced in Fig. 15i and the result has shown that the superhydrophobic silver-containing coating reduced the number of viable bacteria on steel by one unit in the logarithmic scale, i.e., by 88%. Xue et al.[226] adopted the same reduction method to produce Ag NPs on cotton fibers. After modification of silver-containing fiber with hexadecyltrimethoxysilane let to superhydrophobic cotton textiles. Antibacterial activity of fabric samples was determined in terms of inhibition zone formed on agar medium. Fig. 15f shows that the normal cotton samples did not show any antibacterial activity. The silver modified cotton textiles killed all the bacteria under and around them.

In summary, to some extent, those strategies are useful in anti-bacteria, but a few of them are also associated with shortcomings related to stability, toxicity or short lifespan.[222] Better materials should be taken into account or new strategies need to be developed to solve these problems in the future.

Transparency and anti-reflection

Transparent superhydrophobic nanocoating has broad application prospect including windows, eyeglasses, camera lenses and solar cell system, etc..[227] Transparency will be reduced with surface roughness increases because the light scattering.[228] But, it has been suggested that the optimization of the surface roughness is important factor for creating the superhydrophobic surface.[229] That is to say, the two properties (superhydrophobicity and transparency) are generally competitive.[230] According to Rayleigh scattering theory[231], Raleigh scattering is negligible in the visible region when the roughness is far less than the irradiated light wavelength. However, the Mie scattering occurs when roughness size is comparable or greater than irradiated light wavelength.[232] In this case, the wide range of irradiated light is scattered by the structured surface depending upon surface roughness, incident angles, and differences of refractive indices between the air and surface. Theoretical computation results indicate that Mie scattering increases exponentially by increasing the roughness. Based on the above researches, roughness at the scale of sub-100-nm would be more conductive to achieve higher

transparency.[228]

Si/SiO$_2$ based nanocoating is endowed with excellent optical property and the convenient further chemical treatment and is easy to control coating thickness and roughness. Because of this
5 advantage, Si/SiO$_2$ based material received a lot of attention in this research field. Xu et al.[233] successfully fabricated highly transparent and durable superhydrophobic hybrid nanoporous coatings (Fig. 15g) using a liquid polysiloxane (PSO) containing SiH and SiCH=CH$_2$ groups as precursors and methyl-terminated
10 poly(dimethylsiloxane)s (PDMS) as porogens via a simple solidification-induced phaseseparation method. Wang et al.[234] reported the fabrication of superhydrophobic, highly transparent, and stable organic-inorganic composite nanocoating by an elegant sol-gel dip-coating method. The tetraethylorthosilicate
15 (TEOS) was used as precursors to obtain the silica sol. Then different amounts of γ-aminopropyltriethoxysilane（APS）used to aggregate the silica colloid particles in the prepared sols. After dip-coating process and surface fluorination, the superhydrophobic transparent nanocoating was formed (Fig. 15h).
20 In the case of organic materials, polymer nanocoatings are always largely flexible and have controllable stiffness comparing to their inorganic counterparts. For example, superhydrophobic coating on poly(methyl methacrylate) (PMMA) using a dry etching with CF$_4$ plasma and a subsequent hydrolysis process with water
25 immersion had been papered.[235] High transmittance (> 95%) was achieved for the prepared coating surfaces.

Reflective light on the surface will cause two harms: energy loss an imaging interference.[236] Anti-reflection is absolutely important to our daily life. Inspired by moth-eyes[237, 238], anti-
30 reflective micro-nanostructures with a period smaller than the irradiated light wavelength could lead to an effective refractive-index gradient between air and the substrate. Based on these theories, a number of considerable micro-nanostructures have been designed.[239-241, 82] Combined with transparency and self-
35 cleaning, the application of transparent superhydrophobic nanocoating on solar cells[242, 243] has been noted because of it could enhance optical absorption and remove the pollutants on the surface.
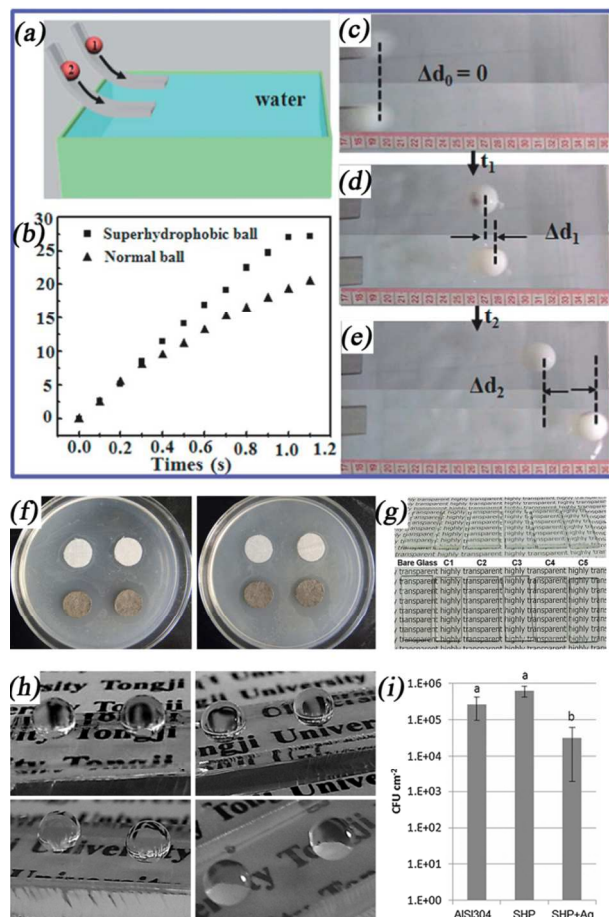
40 **Fig. 15** (a) Schematic illustration of the movement of superhydrophobic and normal balls; (b) The position of the superhydrophobic and normal balls versus time; Photographs of the two balls moving on water surface after rolling down a channel from the same height at (c) t = 0 s (the two balls move horizontally, the position difference is Δd$_0$ = 0), (d) t$_1$ = 0.61 s, (e) t$_2$ = 1.11 s.[216] (i)
45 Bacterial cell counts (CFU cm^{-2}) on coupons of stainless steel as uncoated (AISI304), or coated with superhydrophobic (SHP) or superhydrophobic silver-containing coating (SHP + Ag) after exposed to a mixture of three bacterial strains for 1 day at 25 °C. The number of adhered bacteria was determined by cultivations from 3 parallel specimens. Bars show standard
50 deviations. Values with the same letter are not significantly (P ≤ 0.05) different from each other.[83] (f) Antibacterial activity of (left) normal cotton (the upper two) and Ag NP modified cotton (the lower two) textiles, and (right) normal cotton (the upper two) and hydrophobized Ag NP modified cotton (the lower two) textiles.[226] (g) Angled (upper) and front (lower) photographs of bare glass
55 and the different PDMS viscosities of the C1−C5 coatings.[233] (h) Optical images of glass substrates with superhydrophobic coatings from sols containing 0.36% APS, 0.48% APS, 0.6% APS, and 0.72% APS (left to right, up to down).[234] (a-e) Reproduced with permission from [216], Copyright (2014) The Royal Society of Chemistry. (i) Reproduced with permission from [83],
60 Copyright (2014) Elsevier. (f) Reproduced with permission from [226], Copyright (2012) Elsevier. (g) Reproduced with permission from [233], Copyright (2014) American Chemical Society. (h) Reproduced with permission from [234], Copyright (2010) American Chemical Society.

Others applications

65 Others applications about superhydrophobic nanocoating are reported in the last three years.[55, 244-246] Li et al.[247] fabricated successfully tunable adhesive superhydrophobic ZnO coating

based on the design of heterogeneous chemical composition on the ZnO NP surfaces by simply spraying ZnO nanoparticle (NP) suspensions onto desired substrates. On the basis of the different adhesive forces of the tunable adhesive superhydrophobic
5 surfaces, the selective transportation of microdroplets with different volumes was achieved for the first time. This tunable adhesive superhydrophobic nanocoating may open a door to selective water droplet transportation, biomolecular quantitative detection and droplet-based biodetection. Membrane distillation
10 (MD) is an emerging process that can utilize low-grade or waste heat to generate high-quality water from impaired water with high recovery. Wang and co-workers[248] developed a strategy to construct superhydrophobic composite nanofiber membranes produced by electrospinning which could be used in MD.
15 Superhydrophobic coatings also could be potentially used in crystals assembly. Song et al.[249] demonstrated a facile approach for achieving three-dimensional colloidal PCs with narrow stopbands on low-adhesive superhydrophobic substrates. Low-adhesive superhydrophobic coating caused many properties
20 profits, such as perfectly ordered assembly structure, large-scale crack elimination, decreased void fraction, and sufficient thickness of the resultant colloidal PCs. Inspired by the air sacs found in aquatic plants such as lotus, Lee et al.[250] mparted high buoyancy to free-standing superhydrophobic films by embedding
25 nanoparticle-shelled bubbles in the structure. These highly buoyant superhydrophobic films stay afloat on water surface while carrying a load that is more than 200 times their own weight which can potentially be used for the fabrication of lightweight materials.

30 Conclusions and outlook

Although superhydrophobicity and nanotechnology are both recently developed concepts, they have already become important to a lot of research and will be potentially important to people's life. The combination of them has prompted the creation of the
35 multifunction superhydrophobic nanocoating, which play important roles in many practical applications. In this review, we give a summary of the fundamental theories and recent progress in synthesis of a range of different superhydrophobic nanocoating using a wide variety of materials, fabrication methodologies. The
40 application and special performance of superhydrophobic nanocoating also have been discussed. Although, tremendous great efforts have been accomplished in this field during the past years, it should be pointed out that the investigations still retain many challenges, and some of the problems still need to be
45 solved for further study.

Indeed, these are the respective advantages of different materials on artificial superhydrophobic nanocoating field. Carbon-based, Silica-based inorganic materials usually have excellent chemical resistance in both acid and alkaline conditions.
50 Metallic oxide, such as ZnO, TiO_2, SnO_2, are common materials exhibiting a wide range of surface morphologies like nanorods, nanotube and nanoneedles. Compared with inorganic coating, polymers of high transparency have their own advantages such as simple fabrication, structural flexibility and controllable thickness.
55 However, what worthy of our attention are disadvantages of various materials, for example, the problem of metallic oxide corrosion, the high price of carbon nanotube or grapheme, and the

toxicity of organic polymers. The most important thing for researchers is to figure out some feasible solutions in the future.
60 Out of the original mode of thinking, new materials may open a fire-new door for us. Metal-organic frameworks (MOFs), natural protein, organoclay[251-254] all have attracted some interest. Seeking answers to natural would be another nice solution. No matter animalia or plantae, a number of new biological models[255-259] had
65 come into our view. What is more, new biological models would contribute to establish new theoretical model.

And it does, it is a pressing need to establish new theoretical model, or say it is crucial to develop the corresponding theories. Up to now, the theoretical researches of mechanism of
70 superhydrophobic nanocoating are limited to the classical models, Wenzel and Cassie models, which are only suitable for special conditions because of the limitation of the Wenzel and Cassie models by themselves[260-261]. Furthermore, it is not yet fully known how a wetting transition would occur, what role contact
75 line plays and what essence of energy barrier is.[262-264] These questions really have enormous industrial value to optimize the surface morphology. And, to some extent, such a field has encountered some bottlenecks in applications due to lack of guidance from corresponding advanced theories.
80 To be frank, as to application, there are two key points needed to be solved: large-scale preparation and the binding strength between nanocoating and substrates. Of course, mechanical and thermal stability, robustness, and self-healing ability of the superhydrophobic nanocoating are very important for practical
85 applications as well. We stand a chance to make breakthroughs in potential application based on the predecessors' researches. Combining of two or more system members is the routine thoughts. Perhaps, superhydrophobic nanocoating could be used into control other substances' synthesis or assembly.[249] Also,
90 some researchers started to investigate the behaviors of special droplets, such as supercooled water, condensed water or magnetic droplets[265-267], on superhydrophobic surfaces.

All in all, the extreme goal for artificial superhydrophobic nanocoating is the perfect integration of novel structural and
95 functional properties with long service life. Scients expect that, with further development, superhydrophobic nanocoatings need to the cooperation of interfacial science and other fields, such as biology, physics, medicine, and thus hold great promise for multidisciplinary applications. With ever-increasing number of
100 scientists focused on this area, we believe an exciting future in synthesis, theory and commercialization of superhydrophobic nanocoatings field.

Acknowledgements

Notes and references

ᵃ Hubei Collaborative Innovation Centre for Advanced Organic Chemical Materials and Ministry of Education Key Laboratory for the Green Preparation and Application of Functional Materials, Hubei University, Wuhan 430062, People's Republic of China. Fax: 0086-931-8277088; Tel: 0086-931-4968105; E-mail: zguo@licp.cas.cn (GUO)
ᵇState Key Laboratory of Solid Lubrication, Lanzhou Institute of Chemical Physics, Chinese Academy of Sciences, Lanzhou 730000, People's Republic of China

1   W. Hannah and P. B. Thompson, *J. Environ. Monit.*, 2008, **10**, 291.
2   D. G. Thomas, F. Klaessig and N. A. Baker, *Wiley Interdiscip. Rev. Nanomed. Nanobiotechnol.*, 2011, **3**, 511.
3   H. Ramsurn, R. B. Gupta, ACS Sustainable Chem. Eng. 1 (2013) 779-797.
4   Z. G. Guo, F. Zhou, J. C. Hao, Y. M. Liang, W. M. Liu and W. T. S. Huck, *Appl. Phys. Lett.*, 2006, **89**, 081911.
5   C. R. Crick and I. P. Parkin, *Chem. Eur. J.*, 2010, **16**, 3568.
6   B. Bhushan and Y. C. Jung, *Prog. Mater. Sci.*, 2011, **56**, 1.
7   Z. G. Guo, F. Zhou, J. C. Hao and W. M. Liu, *J. Colloid Interface Sci.*, 2006, **303**, 298.
8   J. Adams and D. Pendlebury, *Global Research Report: Materials Science and Technology*, Thomson Reuters ScienceWatch, 2011.
9   G. Y. Wang, Z. G. Guo and W. M. Liu, *J. Bionic Eng.*, 2014, **11**, 325.
10 H. J. Li, X. B. Wang, Y.L. Song, Y. Q. Liu, Q. S. Li, L. Jiang and D. B. Zhu, *Angew. Chem. Int. Ed.*, 2001, **40**, 1743.
11 K. Lum, D. Chandler and J. D. Weeks, *J. Phys. Chem. B*, 1999, **103**, 4570.
12 E. Bittoun and A. Marmur, *Langmuir*, 2012, **28**, 13933.
13 L. Feng, S. H. Li, Y. S. Li, H. J. Li, L. J. Zhang, J. Zhai, Y. L. Song, B. Q. Liu, L. Jiang and D. B. Zhu, *Adv. Mater.*, 2002, **14**, 1857.
14 K. Koch, B. Bhushan, Y. C. Jung and W. Barthlott, *Soft Matter*, 2009, **5**, 1386.
15 J. B. Boreyko, C. H. Baker, C. R. Poley and C. H. Chen, *Langmuir*, 2011, **27**, 7502.
16 T. Verho, J. T. Korhonen, L. Sainiemi, V. Jokinen, C. Bower, K. Franze, S. Franssila, P. Andrew, O. Ikkala and R. H. A. Ras, *Proc. Natl. Acad. Sci. USA*, 2012, **109**, 10205.
17 R. N. Wenzel, *Ind. Eng. Chem.*, 1936, **28**, 988.
18 A. B. D. Cassie and S. Baxter, *Trans. Faraday Soc.*, 1944, **40**, 546.
19 Z. G. Guo, W. M. Liu and B. L. Su, *J. Colloid Interface Sci.*, 2011, **353**, 335.
20 A. Marmur, *Soft Matter*, 2012, **8**, 6867.
21 Z. Huan, Z. G. Guo and W. M. Liu, *Chem. Commun.*, 2014,**50**, 3900.
22 D. Que′re′, *Rep. Prog. Phys.*, 2005, **68**, 2495.
23 B. Wang, Y. B. Zhang, L. Shi, J. Li and Z. G. Guo, *J. Mater. Chem.*, 2012, **22**, 20112.
24 J. Xu and Z. G. Guo, *J. Colloid Interface Sci.*, 2013, **406**, 1.
25 L. Zhai, M. C. Berg, F. C. Cebeci, Y. Kim, J. M. Milwid, M. F. Rubner and R. E. Cohen, *Nano Lett.*, 2006, **6**, 1213.
26 B. H. Lamoral, *Ann. Natal Mus.*, 1968, **20**, 151.
27 A. K. Kota, G. Kwon and A. Tuteja, *NPG Asia Materials*, 2014, **6**, DOI:10.1038/am.2014.34.
28 K. Liu, X. Yao and L. Jiang, *Chem. Soc. Rev.*, 2010,**39**, 3240.
29 Z. G. Guo, F. Zhou, J. C. Hao and W. M. Liu, *J. Am. Chem. Soc.*, 2005, **127**, 15670.
30 M. N. Valipour, F. C. Birjandi and J. Sargolzaei, *Colloids and Surfaces A: Physicochem. Eng. Aspects*, 2014, **448**, 93.
31 Z. G. Guo, W. M. Liu and B. L. Su, *Appl. Phys. Lett.*, 2008, **93**, 201909.
32 B. Wang, J. Li, G. Y. Wang, W.X. Liang, Y. B. Zhang, L. Shi, Z. G. Guo and W. M. Liu, *ACS Appl. Mater. Interfaces*, 2013, **5**, 1827.
33 A. W. Adamson and A. P. Gast, *Physical Chemistry of Surfaces*, 6th ed. New York: John Wiley-Interscience, 1997.
34 A. Marmur, *Langmuir*, 2003, **19**, 8343.
35 C. G. L. Furmidge, *J. Colloid Sci.*, 1962, **17**, 309.
36 J. Genzer and K. Efimenko, *Science*, 2000, **290**, 2130.
37 T. Nishino, M. Meguro, K. Nakamae, M. Matsushita and Y. Ueda, *Langmuir*, 1999, **15**, 4321.
38 C. Neinhuis and W. Barthlott, *Ann. Bot.*, 1997, **79**, 667.
39 W. Barthlott and C. Neinhuis, *Planta*, 1997, **202**, 1.
40 M. M. Xiang, A. Wilhelm and C. Luo, *Langmuir*, 2013, **29**, 7715.
41 L. Mammen, X. Deng, M. Untch, F. Leroy, et al., *Langmuir*, 2012, **28**, 15005
42 A. H. F. Wu, K. L. Cho, I.I. Liaw, G. Moran, N. Kirby and R.N. Lamb, *Faraday Discuss.*, 2010, **146**, 223.
43 M. E. Yazdanshenas and M. Shateri-Khalilabad, *Ind. Eng. Chem. Res.*, 2013, **52**, 12846.
44 S. A. Seyedmehdi, H. Zhang and J. Zhu, *Appl. Surf. Sci.*, 2012, **258**, 2972.
45 K. Q Li, X. R Zeng, H. Q Li, X. J Lai and H. Xie, *Colloids and Surfaces A: Physicochem. Eng. Aspects*, 2014, **445**, 111.
46 J. P Zhang, A. Q. Wang and S. Seeger, *Adv. Funct. Mater.*, 2014, **24**, 1074.
47 H. Zhou, H. Xa. Wang, H. T Niu, A. Gestos, X. G. Wang, T. Lin, *Adv. Mater.*, 2012, **24**, 2409.
48 S. E. Lee, D. J Lee, P. Lee, S. H. Ko, S.S. Lee and S.U. Hong, *Macromol. Mater. Eng.*,2013, **298**, 311.
49 S. G. Lee, D. S. Ham, D. Y. Lee, H. Bong, K. Cho, *Langmuir*, 2013, **29**, 15051.
50 G. Hayase, K. Kanamori, G. Hasegawa, A. Maeno, H. Kaji and K. i Nakanishi, *Angew. Chem.*, 2013, **125**, 10988.
51 B. G. Choi and H. S. Park, *J. Phys. Chem. C*, 2012, **116**, 3207.
52 J. S. Lee, J. C Yoon and J. H. Jang. *J. Mater. Chem. A*, 2013, **1**, 7312.
53 X. T. Zhu, Z. Z. Zhang, B. Ge, X. H. Men and X. Y. Zhou, *Colloids and Surfaces A: Physicochem. Eng. Aspects*, 2014, **444**, 252.
54 Y. Sohn, D. Kim, S. Lee, M. Yin, J. Y. Song, et al., *J. Mater. Chem. A*, 2014, **2**, 11465.
55 J. Chapman, F. Regan, *Adv. Eng. Mater.*, 2012, **14**, B175.
56 J. S. Liang, D. Li, D. Z. Wang, K. Y. Liu and L. Chen, *Appl. Surf. Sci.*, 2014, **293**, 265.
57 Z. X. She, Q. Li , Z. W. Wang, C. Tan, J. C. Zhou and L. Q. Li, *Appl. Surf. Sci.*, 2012, **263**, 297.
58 M. Macias-Montero, A. Borras, P. Romero-Gomez, J. Cotrino et al., *Plasma Process. Polym.*, 2014, **11**, 164.
59 S. Peng, D. Tian, X. J. Yang and W. L. Deng, *ACS Appl. Mater. Interfaces* 2014, **6**, 4831.
60 X. M. Bao, J. F. Cui, H. X. Sun, W.D. Liang, Z. Q. Zhu et al., *Appl. Surf. Sci.*, 2014, **303**, 473.
61 J. Li, L. Shi, Y. Chen, Y. B. Zhang, Z. G. Guo, B.L. Su, W. M Liu, *J. Mater. Chem.*, 2012, **22**, 9774.
62 L. Gao, J. Zhuang, L. Nie, J. Zhang, Y. Zhang, N. Gut, et al., *Nat. Nanotechnol.*, 2007, **2**, 577.
63 N. Wang, L. Zhu, M. Wang, D. Wang and H. Tang, *Ultrason. Sonochem.*, 2010, **17**, 78.
64 D. Hong, I. Ryu, H. Kwon, J.J. Lee and S. Yim, *Phys. Chem. Chem. Phys.*, 2013, **15**, 11862.
65 Z. Q. Yuan, J. P. Bin, X. Wang, Q. L. Liu, D. J. Zhao, H. Chen and H. Y. Jiang, *Polym. Eng. Sci.*, 2012, **52**, 2310.
66 E. Huovinen, L. Takkunen, T. Korpela, M. Suvanto, T. T. Pakkanen and T. A. Pakkanen, *Langmuir*, 2014, **30**, 1435.
67 D. Nyström, J. Lindqvist, E. Östmark, P. Antoni, A. Carlmark, A. Hult and E. Malmström, *AM&I*, 2009, **1**, 816.
68 H. Li, Y. H. Zhao and X. Y. Yuan, *Soft Matter*, 2013, **9**, 1005.
69 N. A. Ivanovaa and A. B. Philipchenkob, *Appl. Surf. Sci.*, 2012, **263**, 783.
70 Y. Q. Qing, Y. S. Zheng, C. B. Hu, Y. Wang, Y. He, et al., *Appl. Surf. Sci.*, 2013, **285**, 583.
71 R. P. S. Chakradhar, G. Prasad and P. Bera, C. Anandan, *Appl. Surf. Sci.*, 2014, **301**, 208.
72 Y. Zhang, J.L. Li, F.Z. Huang, S.K. Li, Y.H. Shen, A.J. Xie, et al., *Appl Phys A*, 2013, **110**, 397.
73 Y. C. Tang, J. Yang, L. T Yin, B. B. Chen, H. Tang, C. Liu and C. S. Li, *Colloids and Surfaces A: Physicochem. Eng. Aspects*, 2014, **459**, 261.
74 W. Y. Gan, S. W. Lam, K. Chiang, R. Amal, H. J. Zhao and M. P. Brungs, *J. Mater. Chem.*, 2007, **17**, 952.
75 X. T. Zhang, H. Kono, Z. Y. Liu, S. Nishimoto, D. A. Tryk, T. Murakami, H. Sakai, M. Abe and A. Fujishima, *Chem. Commun.*, 2007, **46**, 4949.
76 W. X. Hou and Q. H. Wang, *Langmuir*, 2007, **23**, 9695.
77 X. T. Zhang, M. Jin, Z. Y. Liu, D. A. Tryk, S. Nishimoto, T. Murakami and A. Fujishima, *J. Phys. Chem. C*, 2007, **111**, 14521.
78 J. X. Wang, Y. Q. Wen, J. P. Hu, Y. L. Song and L. Jiang, *Adv. Funct. Mater.*, 2007, **17**, 219.
79 H. F. Hoefnagels, D. Wu, G. With and W. Ming, *Langmuir*, 2007, **23**, 13158.
80 Z. B. Huang, Y. Zhu, J. H. Zhang and G. F. Yin, *J. Phys. Chem. C*, 2007, **111**, 6821.
81 Y. Li, G. T. Duan, W. P. Cai, *J. Colloid Interface Sci.*, 2007, **314**, 615.
82 X. X. Zhang, S. Cai, D. You, L. H. Yan, H. B. Lv, X. D. Yuan and B. Jiang, *Adv. Funct. Mater.*, 2013, **23**, 4361.
83 S. Heinonen, E. Huttunen-Saarivirta, J. P. Nikkanen, et al., *Colloids and Surfaces A: Physicochem. Eng. Aspects*, 2014, **453**, 149.
84 J. Lin, H. Chen, T. Fei, et al., *Colloids and Surfaces A: Physicochem. Eng. Aspects*, 2013, **421**, 51.
85 X. B. Yan, B. K. Tay, Y. Yang and Y. K. Po, *J. Phys. Chem. C*, 2007, **111**, 17254.

86   L. J. Ci, R. Vajtai and P. M. Ajayan, *J. Phys. Chem. C*, 2007, **111**, 9077.

87   S. H. Li, H. B. Xie, S.B. Zhang and X. H. Wang, *Chem. Commun.*, 2007, **46**, 4857.

88   S. C. Ramos, G. Vasconcelos, E. F. Antunes, A. O. Lobo, V. J. Trava-Airoldi and E. J. Corat, *Surf. Coating. Technol.*, 2010, **204**, 3073.

89   L. Y. Meng and S. J. Park, *Mater. Chem. Phys.*, 2012, **132**, 324.

90   J. Pan, X. Song, J. Zhang, H. Shen and Q. Xiong, *J. Phys. Chem.*, 2011, **115**, 22225.

91   J. Xiong, S. N. Das, B. Shin, J. P. Kar, J. H. Choi and J. M. Myoung, *J. Colloid Interface Sci.*, 2010, **350**, 344.

92   A. Pakdel, C. Zhi, Y. Bando, T. Nakayama and D. Golberg, *ACS Nano*, 2011, **5**, 6507.

93   L. Zhang and J. Sun, *Macromolecules*, 2010, **43**, 2413.

94   A. Hozumi, D.F. Cheng and M. Yagihashi, *J. Colloid Interface Sci.*, 2011, **353**, 582.

95   Y. Yoo, J. B. You, W. Choi and S. G. Im, *Polym. Chem.*, 2013, **4**, 1664

96   X. Liu, B. Dai, L. Zhou andJ. Sun, *J. Mater. Chem.*, 2009, **19**, 497.

97   A. Pakdel, Y. Bando and D. Golberg, *Langmuir*, 2013, **29**, 7529.

98   S. Rezaei, I. Manoucheri, R. Moradian and B. Pourabbas, *Chem. Eng. J.*, 2014, **252**, 11.

99   Z. Shen, C. Hou, S. Liu, et al., *J. Appl. Polym. Sci.*, 2014, **131**, DOI: 10.1002/app.40400.

100 W. C. Wu, X.L. Wang, X.J. Liu and F. Zhou, *ACS Appl. Mater. Interfaces*, 2009, **8**, 1656.

101 X. L. Wang, H. Y. Hu, Q. Ye, T. T Gao, F. Zhou and Q. J. Xue, *J. Mater. Chem.*, 2012, **22**, 9624.

102 Y. Li, S. S. Chen, M. C. Wu and J. Q. Sun, *Adv. Mater.*, 2014, **26**, 3344.

103 Z. F Wua, H. Wang, M. Xue, X. Y. Tian, X. Z. Ye, H. F. Zhou and Z. Y. Cui, *Compos. Sci. Technol.*, 2014, **94**, 111.

104 E. K. Kim, J. Y. Kim and S. S. Kim, *J. Solid State Chem.*, 2013, **197**, 23.

105 J. Y. Kim, E. K. Kim and S. S. Kim, *J. Colloid Interface Sci.*, 2013, **392**, 376.

106 Y. Guo, D. Tang and Z. L. Gong, *J. Phys. Chem. C*, 2012, **116**, 26284.

107 E. Burkarter, C. Saul, F. Thomazi, N. Cruz, L. Roman and W. Schreiner, *Surf. Coat. Technol.*, 2007, **202**, 194.

108 H. Yoon, J. H. Park and G. H. Kim, *Macromol. Rapid Commun.*, 2010, **31**, 1435.

109 S. T. Yohe and M. W. Grinstaff, *Chem. Commun.*, 2013, **49**, 804.

110 I. Sas, R. E. Gorga, J. A. Joines and K. A. Thoney, *J. Polym. Sci., Part B: Polym. Phys.*, 2012, **50**, 824.

111 A. Kulkarni, V. A. Bambole and P. A. Mahanwar, *Polym. Plast. Technol. Eng.*, 2010, **49**, 427.

112 S. Michielsen, H. J. Lee, *Langmuir*, 2007, **23**, 6004.

113 Y. Y. Liu, R. H. Wang, H. F. Lu, L. Li, Y. Y. Kong, K. H. Qi and J. H. Xin, *J. Mater. Chem.*, 2007, **17**, 1071.

114 M. Ma, R. M. Hill, J. L. Lowery, S. V. Fridrik and G. C. Rutledge, *Langmuir*, 2005, **21**, 5549.

115 Y. Jiang, J. Zhao andJ. Zhai, Angew. Chem., Int. Ed., 2004, 43, 4338.

116 M. R. Karim and M. S. Islam, *J. Nanomater.*, 2011, **2011**, 5.

117 H. S. Lim, J. H. Baek, K. Park, H. S. Shin, J. Kim and J. H. Cho, *Adv. Mater.*, 2010, **22**, 2138.

118 D. Cho, H. Zhou, Y. Cho, D. Audus and Y. L. Joo, *Polymer*, 2010, **51**, 6005.

119 S. H. Park, S. M. Lee, H. S. Lim, J. T. Han, D. R. Lee, H. S. Shin, Y. Jeong, J. Kim and J. H. Cho, *ACS Appl. Mater. Interfaces*, 2010, **2**, 658.

120 M. Sun, X. Li, B. Ding, J. Yu and G. Sun, *J. Colloid Interface Sci.*, 2010, **347**, 147.

121 P. Muthiah, S. H. Hsu and W. Sigmund, *Langmuir*, 2010, **26**, 12483.

122 V. A. Ganesh, A. S. Nair, H. K. Raut, T. T. Yuan Tan, et al., *J. Mater. Chem.*, 2012, **22**, 18479.

123 S. Wang, Y. B. Yang, Y. Zhang, X. L. Fei, C. Zhou, et al., *J. Appl. Polym. Sci.*, 2014, **131**, DOI: 10.1002/APP.39735.

124 F. O. Ochanda, M. A. Samaha, H. V. Tafreshi, G. C. Tepper and M. Gad-el-Hak, *J. Appl. Polym. Sci.*, 2012, **123**, 1112.

125 A. Safaee, D. K. Sarkar and M. Farzaneh, *Appl. Surf. Sci.*, 2008, **254**, 2493.

126 N. Vourdas, A. Tserepi, A. G. Boudouvis and E. Gogolides, *Microelectron. Eng.*, 2008, **85**, 1124.

127 H. C. Shin and M. L. Liu, *Chem. Mater.*, 2004, **16**, 5460.

128 X. Zhang, F. Shi, X. Yu, H. Liu, Y. Fu and Z. Q. Wang, *J. Am. Chem. Soc.*, 2004, **126**, 3064.

129 J. T. Han, Y. Jang, D. Y. Lee, J. H. Park, S. H. Song and D. Y. Ban, *J. Mater. Chem.*, 2005, **15**, 3089.

130 E. Hosono, S. Fujihara, I. Honma and H. S. Zhou, *J. Am. Chem. Soc.*, 2005, **127**, 13458.

131 Z. X. She, Q. Li, Z. W. Wang, C. Tan, J. C. Zhou and L. Q. Li, *Surf. Coat. Technol.*, 2014, **251**, 7.

132 Q. Y. Yu, Z. X. Zeng, W. J. Zhao, M. H. Li, X. D. Wu and Q. J. Xue, *Colloids and Surfaces A: Physicochem. Eng. Aspects*, 2013, **427**, 1.

133 Z. Chen, L. M. Hao, M. M. Duan and C. L. Chen, *Appl Phys A*, 2013, **111**, 581.

134 Z. W. Wang, Q. Li, Z. X. She, F. N. Chen and L. Q. Li, *J. Mater. Chem.*, 2012, **22**, 4097.

135 M. Wolfs, T. Darmanin and F. Guittard, *Eur. Polym. J.*, 2013, **49**, 2267.

136 X. T. Zhang, J. Liang, B. X. Liu and Z. J. Peng, *Colloids and Surfaces A: Physicochem. Eng. Aspects*, 2014, **454**, 113.

137 M. Wolfs, T. Darmanin and F. Guittard, *Soft Matter*, 2012, **8**, 9110.

138 R. Gao, Q. Liu, J. Wang, X. F. Zhang, W. L. Yang, et al., *Chem. Eng. J.*, 2014, **241**, 352.

139 A. K. Sinha, M. Basu, M. Pradhan, S. Sarkar and T. Pal, *Chem.-Eur. J.*, 2010, **16**, 7865.

140 C. Mondal, M. Ganguly, A. K. Sinha, J. Pal and T. Pal, *RSC Adv.*, 2013, **3**, 5937.

141 Z. W. Hu and W. Li, *J. Colloid Interface Sci.*, 2012, **376**, 245.

142 L. Yao, M. Zheng, C. Li, et al., *Nanoscale Res. Lett.*, 2012, **7**, 1.

143 S. L. Wang, C. Y. Wang, C. Y. Liu, M. Zhang, H. Ma and J. Li, *Colloids and Surfaces A: Physicochem. Eng. Aspects*, 2012, **403**, 29.

144 Y. Q. Gao, I. Gereige, A. E. Labban, D. Cha, et al., *ACS Appl. Mater. Interfaces*, 2014, **6**, 2219.

145 T. H. Li, Q. G. Li, J. Yan and F. Li, *Dalton Trans.*, 2014, **43**, 5801.

146 Z. J. Wang, J. H. Gong, J. H. Ma and J. Xu , *RSC Adv.*, 2014, **4**, 14708.

147 T. Zhang, H.Q Yan, Z. P Fang, Y. P. E, T. Wu and F. Chen, *Appl. Surf. Sci.*, 2014, **309**, 218.

148 J. Xua, J. L. Xu, Y. Cao, X. B. Ji and Y. Y. Yan, *Appl. Surf. Sci.*, 2013, **286** 220.

149 J. F. Ou, W. H. Hu, M. S. Xue, F. J. Wang and W. Li, *ACS Appl. Mater. Interfaces*, 2013, **5**, 9867.

150 H. J. Choi, J. H. Shin, S. Choo, J. Kim and H. Lee, *J. Mater. Chem. A*, 2013, **1**,8417.

151 L. P. Yang, A. Raza, Y. Si, X. Mao, Y. W. Shang, B. Ding, et al., *Nanoscale*, 2012, **4**, 6581.

152 M. Laurenti, V. Cauda, R. Gazia, M. Fontana, V. F. Rivera, S. Bianco and G. Canavese, *Eur. J. Inorg. Chem.*, 2013, **14**, 2520.

153 X. Deng, L. Mammen, H. J. Butt and D. Vollmer, *Science*, 2012, **335**,67.

154 L. B. Boinovich, A. G. Domantovskiy, A. M. Emelyanenko, A. S. Pashinin, et al., *Appl. Mater. Interfaces*, 2014, 6, 2080.

155 J. L. Yong, F. Chen, Q. Yang, D. S. Zhang, G. Q. et al., *J. Phys. Chem. C*, 2013, **117**, 24907.

156 C. F. Wang, H. Y. Chen, S. W. Kuo, Y. S. Lai and P. F. Yang, *RSC Adv.*, 2013, **3**, 9764.

157 Y. C. Lin, S. H. Hsu and Y. C. Chung, *Surf. Coat. Technol.*, 2013, **231**,501.

158 S. Kato and A. Sato, *J. Mater. Chem.*, 2012, **22**, 8613.

159 S. V. Gnedenkov, V. S. Egorkin, S. L. Sinebryukhov, I. E. Vyaliy, A. S. Pashinin, A. M. Emelyanenko and L. B. Boinovich, *Surf. Coat. Technol.*, 2013, **232**, 240.

160 X. Y. Chen, J. H. Yuan, J. Huang, K. Ren, Y. Liu, S.Y. Lu and H. Li, *Appl. Surf. Sci.*, 2014, **311**, 864.

161 K. P. Rao, M. Higuchi, K. Sumida, S. Furukawa, J. Duan and S. Kitagawa, *Angew. Chem. Int. Ed.*, 2014, **53**, 1.

162 H. Teisala, M. Tuominen, M. Aromaa, J.M. Mäkelä, M. Stepien, J. J. Saarinen, M. Toivakka and J. Kuusipalo, *Surf. Coat. Technol.*, 2010, **205**, 436.

163 B. Wang, W. X. Liang, Z. G Guo and W. M. Liu, *Chem. Soc. Rev*, 2015, **44**, 336.

164 D. M. Zang, C. X. Wu, R. W. Zhu, W. Zhang, X. Q. Yu, Y. F. Zhang, *Chem. Commun.*, 2013, **49**, 8410

165 C. R. Gao, Z. X. Sun, K. Li, Y. N. Chen, Y. Z. Cao, et al., *Energy Environ. Sci.*, 2013, **6**, 1147.

166 C. R. Crick, J. A. Gibbins and I. P. Parkin, *J. Mater. Chem. A*, 2013, **1**, 5943.

167 D. D. Nguyen, N. H. Tai, S.B. Leea and W,S, Kuo, *Energy Environ. Sci.*, 2012, **5**, 7908.

168 Q. Zhu, Y. Chu, Z.K. Wang, N. Chen, L. Lin, F.T. Liu and Q.M. Pan, *J. Mater. Chem. A*, 2013, **1**, 5386.

169 A. M. A. Mohamed, A. M. Abdullah and N. A. Younan, *Arabian J. Chem.*, 2014, DOI: 10.1016/j.arabjc.2014.03.006.

170 Y L. Zhang, H. Xia, E. Kim and H. B. Sun, *J. Polym. Sci., Part B: Polym. Phys.*, 2008, **46**, 1984.

171 Y. Chen, S. G. Chen, F. Yu, W. W. Sun, H. Y. Zhu and Y. S. Yin, *Surf. Interface Anal.*, 2009, **41**, 872.

172 S. M. Li, Y. G. Wang, J. H. Liu and W. Wei, *Acta Phys.-Chim. Sin.*, 2007, **23**, 1631.

173 Y. H. Fan, C. Z. Li, Z. J. Chen and H. Chen, *Appl. Surf. Sci.*, 2012, **258**,6531.

174 T. Ishizaki and M. Sakamoto, *Langmuir*, 2011, **27**, 2375.

175 C. J. Weng, C. H. Chang, C. W. Peng, S. W. Chen, J. M. Yeh, C. L. Hsu and Y. Wei, *Chem. Mater.*, 2011, **23**, 2075.

176 Q.F. Xu and J.N. Wang, *New J. Chem.*, 2009, **33**, 734.

177 W. J. Xu, J. L. Song, J. Sun, Y. Lu and Z. Y. Yu, *ACS Appl. Mater. Interfaces*, 2011, **3**, 4404.

178 Y. Tian, B. Su and L. Jiang, *Adv. Mater.*, 2014, **26**, 6872.

179 A. C. C. de Leon, R. B. Pernites and R.C. Advincula, *ACS Appl. Mater. Interfaces*, 2012, **4**, 3169.

180 N. Wang and D. S. Xiong, *Appl. Surf. Sci.*, 2014, **305**, 603.

181 S. V. Gnedenkov, V. S. Egorkin, S. L. Sinebryukhov, I. E. Vyaliy, A. S. Pashinin, A. M. Emelyanenko, L. B. Boinovich, *Surf. Coat. Technol.*, 2013, **232**, 240.

182 C. S. Liu, F. H. Su, J. Z. Liang and P. Huang, *Appl. Surf. Sci.*, 2014, **258**, 580.

183 Y. Li, L. Li and J. Q Sun, *Angew. Chem. Int. Ed.*, 2010, **49**, 6129.

184 P. Roach, N. Shirtcliffe and M. Newton, *Soft Matter*, 2008, **4**, 224.

185 C. Extrand, *Encyclopedia of Surface and Colloid Science*, 2nd edn (ed. P.Somasundaran), Taylor and Francis, New York, 2006 pp. 5854-5868.

186 J. Genzer and A. Marmur, *MRS Bull.*, 2008, **33**, 742.

187 M. Ma, R. Hill and G. Rutledge, *J. Adhes. Sci. Technol.*, 2008, **22**, 1799.

188 W. S. Tung and W. A. Daoud, *J. Mater. Chem.*, 2011, **21**, 7858.

189 B. Bhushan, Y. C. Jung and K. Koch, *Philos. Trans. R. Soc. A*, 2009, **367**, 1631.

190 L. Gao, T. J. McCarthy and X. Zhang, *Langmuir*, 2009, **25**, 14100.

191 V. A. Ganesh, H. K. Raut, A. S. Naira and S. Ramakrishna, *J. Mater. Chem.*, 2011, **21**,16304.

192 K. Liu, Z. Li, W. Wang and L. Jiang, Appl. Phys. Lett., 2011, 99, 261905.

193 K. Liu and L. Jiang, *Annu. Rev. Mater. Res.*, 2012, **42**, 231.

194 Q. F. Xu, Y. Liu and F. J. Lin, *ACS Appl. Mater. Interfaces*, 2013, **5**, 8915.

195 A. Y. Y. Ho, E. L. Van, C. T. Lim, S. Natarajan, N. Elmouelhi, H. Y. Low, M. Vyakarnam, K. Cooper and I. Rodriguez, *J. Polym. Sci. Part B: Polym. Phys.*, 2014, **52**, 603.

196 W. A. Daoud, *Self-Cleaning Materials and Surfaces: A Nanotechnology Approach*, First Edition. John Wiley & Sons, Ltd. 2013.

197 K. M. Wisdom, J. A. Watson, X. P. Qu, F. J. Liu, G. S. Watson and C. H. Chen, *PNAS*, 2013, **110**, 7992.

198 A. J. Meuler, G. H. McKinley and R. E. Cohen, *ACS Nano*, 2010, **4**, 7048.

199 J. Y Lv, Y. L. Song, L. Jiang and J. J. Wang, *ACS Nano*, 2014, **8**, 3152.

200 C. Y Peng, S. L Xing, Z. Q Yuan, J. Y. Xiao, C. Q. Wang and J. C. Zeng. *Appl. Surf. Sci.*, 2012, **259**, 764.

201 L. Boinovich and A. M. Emelyanenko, *Langmuir*, 2014, **30**, 12596.

202 J. Yang and W. Li. *J. Alloys Compd.*, 2013, **576**, 215.

203 L. L. Cao, A.K. Jones, V. K. Sikka, J. Z. Wu and D. Gao. *Langmuir*, 2009, **25**, 12444.

204 X. M. Li, D. Reinhoudt and M. Crego-Calama, *Chem. Soc. Rev.*, 2007, **36**, 1350.

205 J. B. Boreyko, B. R. Srijanto, T. D. Nguyen, C. Vega, M. Fuentes-Cabrera and C. P. Collier, *Langmuir*, 2013, **29**, 9516.

206 D. Richard and D. Quéré, *Europhys. Lett.*, 2000, **50**, 769.

207 Y. Y. Wang, J. Xue, Q. J. Wang, Q. M Chen and J. F Ding. *ACS Appl. Mater. Interfaces*, 2013, **5**, 3370.

208 L. Zhu, J. Xue, Y. Y Wang, Q. M. Chen, J. F Ding and Q. J Wang. *ACS Appl. Mater. Interfaces*, 2013, **5**, 4053.

209 M. Nosonovsky, V. Hejazi, K. Sobolev and M. Nosonovsky, *Sci. Rep.*, 2013, **3**, 2194.

210 G. McHale, M. I. Newton and N. J. Shirtcliffe , *Soft Matter*, 2010, **6**, 714.

211 B. Bhushan, Langmuir, 2012, **28**, 1698.

212 X. Zhang, F. Shi, J. Niu, Y. G. Jiang and Z. Q. Wang, *J. Mater. Chem.*, 2008, **18**, 621.

213 B. Su, M. Li and Q. H. Lu, *Langmuir*, 2010, **26**, 6048.

214 K. Watanabe, Yanuar and H. Udagawa, *J. Fluid Mech.*, 1999, **381**, 225.

215 K. Moaven, M. Rad and M. Taeibi-Rahni, *J. Alloys Compd.*, 2013, **51**, 239.

216 Z. Y. Deng, W. Wang, L. H. Mao, C. F. Wang and Su Chen, *J. Mater. Chem. A*, 2014, **2**, 4178.

217 H. Y. Dong, M. J. Cheng, Y. J. Zhang, H. Wei and F. Shi, *J. Mater. Chem. A*, 2013, **1**, 5886.

218 J. P. Rothstein, *Annu. Rev. Fluid Mech.*, 2010, **42**, 89.

219 C. Cottin-Bizonne, B. Cross, A. Steinberger and E. Charlaix, *Phys. Rev. Lett.*, 2005, **94**, 056102.

220 C. H. Choi, K. J. A. Westin and K. S. Breuer, *Phys. Fluids*, 2003, **15**, 2897.

221 B. Privett, J. Youn, S. Hong, J. Lee, J. Han, et al., *Langmuir*, 2011, **27**, 597.

222 I. Banerjee, R.C. Pangule and R.S. Kane. *Adv. Mater.*, 2011, **23**, 690.

223 J. M. Schierholz and J. Beuth, *J. Hosp. Infect.*, 2001, **49**, 87.

224 E. Hetrick and M. Schoenfisch, *Chem. Soc. Rev.*, 2006, **35**, 780.

225 W. L. Storm, J. Youn, K. P. Reighard, B. V. Worley, H. M. Lodaya, J. H. Shin and M. H. Schoenfisch, *Acta Biomaterialia*, 2014, **10**, 3442.

226 C. H. Xue, J. Chen, W. Yin, S. T. Jia and J. Z. Ma, *Appl. Surf. Sci.*, 2012, **258**, 2468.

227 Y. Rahmawan, L. B. Xu and S. Yang, *J. Mater. Chem. A*, 2013, **1**, 2955.

228 S. Yu, Z. G Guo and W. M Liu, Chem. Commun., 2014, DOI: 10.1039/c4cc06868h.

229 L.B. Xu, R. G. Karunakaran, J. Guo, S. Yang, *ACS Appl. Mater. Interfaces*, 2012, **4**, 1118

230 D. T. Ge, L. L. Yang, Y. F. Zhang, Y. Rahmawan, S. Yang, *Part. Part. Syst. Char.*, 2014, **31**, 763

231 M. Kerker, *The Scattering of Light and Other Electromagnetic Radiation*, Academic Press, New York, 1969.

232 K. L. Cho, I. I. Liaw, A. H. F. Wu and R. N. Lamb, *J. Phys. Chem. C*, 2010, **114**, 11228.

233 D. Wang, Z. B. Zhang, Y. M. Li and C. H. Xu, *ACS Appl. Mater. Interfaces*, 2014, **6**, 10014.

234 Q. F. Xu, J. N. Wang and K. D. Sanderson. *ACS Nano.*, 2010, **4**, 2201.

235 E. K. Her, T. J. Ko, B. Shin, H. Roh, W. Dai, W. K. Seong, H. Y. Kim, K. R. Lee, K. H. Oh and M. W. Moon. *Plasma Process. Polym.*, 2013, **10**, 481.

236 J. Q. Xi, M. F. Schubert, J. K. Kim, E. F. Schubert, M. Chen, S. Y. Lin and W. Liu, J. A. Smart, *Nat. Photonics*, 2007, **1**, 176.

237 P. B. Clapham and M. C. Hutley, *Nature*, 1973, **244**, 281.

238 M. Ibn-Elhaj and M. Schadt, *Nature*, 2001, **410**, 796.

239 L. G. Xu, L. J. Gao and J. H. He. *RSC Adv.*, 2012, **2**, 12764.

240 Mi. Manca, A. Cannavale, L. D. Marco, A. S. Arico, R. Cingolani and G. Gigli. *Langmuir*, 2009, **25**, 6357.

241 L. G. Xu and J. H. He. *ACS Appl. Mater. Interfaces*, 2012, **4**, 3293.

242 J. Zhu, C. M. Hsu, Z. F. Yu, S. H. Fan and Y. Cui, *Nano Lett.*, 2010, **10**, 1979.

243 S. J. Choi and S. Y. Huh, *Macromol. Rapid Commun.*, 2010, **31**, 539.

244 C. Yang, X. M. Li, J. Gilron, D. f. Kong, Y. Yin, Y. Oren, C. Linder and T. He, *J. Membr. Sci.*, 2014, **456**, 155.

245 A. C. C. Esteves , Y. Luo, M. W. P. van de Put , C. C. M. Carcouët and G. de With, *Adv. Funct. Mater.*, 2014, **24**, 986.

246 Y. Ko, H. Baek, Y. Kim, M. Yoon and J. Cho, *ACS Nano.*, 2013, **7**, 143.

247 J. Li, Z. J. Jing, F. Zha, Y. X. Yang, Q. T Wang and Z. Q Lei, *ACS Appl. Mater. Interfaces*, 2014, **6**, 8868.

248 Y. Liao, R. Wang and A.G. Fane, *Environ. Sci. Technol.*, 2014, **48**, 6335.

249 Y. Huang, J. M. Zhou, B. Su, L. Shi, J. X. Wang, S. R. Chen, L. B Wang, J. Zi, Y. L. Song and L. Jiang, *J. Am. Chem. Soc.*, 2012, **134**, 17053.

250 Y. Choi, T. Brugarolas, S. M. Kang, B. J. Park, B. S. Kim, C. S. Lee and D. Lee, *ACS Appl. Mater. Interface*s, 2014, **6**, 7009.

251 J. G. Nguyen and S. M. Cohen, *J. Am. Chem. Soc.*, 2010, **132**, 4560.

252 T. T. Y. Tan, M. R. Reithofer, E. Y. Chen, A. G. Menon, T. S.A. Hor, J. W. Xu and J. M. Chin, *J. Am. Chem. Soc.*, 2013 ,**135**, 16272.

253 F. Y Dong, G. W. Padua and Y. Wang, *Soft Matter*, 2013, **9**, 5933.

254 A. Steele, I. Bayer and E. Loth, *J. Appl. Polym. Sci.*, 2012, **125**, E445.

255 Y. M. Zheng, X. F. Gao and L. Jiang, *Soft Matter*, 2007, **3**, 178.

256 S. G. Lee, H. S. Lim, D. Y. Lee, D. Kwak and K. Cho, *Adv. Funct. Mater.*, 2013, **23**, 547.

257 A. R. Parker and C. R. Lawrence, *Nature*, 2001, **414**, 33.

258 L. Feng, Y. A. Zhang, J. M. Xi, Y. Zhu, N. Wang, F. Xia and L. Jiang, *Langmuir*, 2008, **24**, 4114.

259 X. F. Gao, X. Yan, X. Yao, L. Xu, K. Zhang, J.H. Zhang, B. Yang and L. Jiang, *Adv. Mater.*, 2007, **19**, 2213.

260 M. Nosonovsky, *Langmuir*, 2007, **23**, 9919.

261 L. C. Gao and T. J. McCarthy, *Langmuir*, 2007, **23**, 3762.

262 D. Wu, S. Z. Wu, Q. D. Chen, Y. L. Zhang, J. Yao, X. Yao, L. G. Niu, J. N. Wang, L. Jiang and H. B. Sun, *Adv. Mater.*, 2011, **23**, 545.

263 M. Ramiasa, J. Ralston, R. Fetzer, R. Sedev, D.M. Fopp-Spori, C. Morhard, C. Pacholski and J. P. Spatz, *J. Am. Chem. Soc.*, 2013, **135**,7159.

264 R. David and A. W. Neumann, *Colloids and Surfaces A: Physicochem. Eng. Aspects*, 2013, **425**, 51.

265 T. Maitra, C. Antonini, M. K. Tiwari, A. Mularczyk, Z. Imeri, P. Schoch and D. Poulikakos, *Langmuir*, 2014, **30**, 10855.

266 Q. Y. Zhang, D. K. Sun, Y. F. Zhang, M. F. Zhu, *Langmuir*, 2014, **30**, 12559

267 J. V. I. Timonen, M. Latikka, L. Leibler, R. H. A. Ras and O. Ikkala, *Science*, 2013, **341**, 253.

5

10

15

20

25

30

35

40

45

50

55

www.rsc.org/xxxxxx

ARTICLE TYPE

Table 1 A summary of various materials in this review used to create superhydrophobic nanocoatings

	Materials	Method	Structure	WCA / SA	Substrate	Ref.
inorganic Silica-based	TEOS, OTES	ultrasound irradiation	micro-nano structure	152.8° ± 2.6 / 8°	cotton fabric	43
	RTV silicone rubber, fluoric NPs	spray/ brush/ dip coating	random	>145°/ ~ 3°	ceramic slab	44
	PDMS, SiO$_2$ NPs,	spray, calcination	hierarchical	153°/ > 5°	slide glass	45
	fluoro-SNs, Krytox	coating spread	nanofilaments	related to thickness	glass slide	46
Carbon-based	graphene, Nafion	supramolecular assembly	petal-like, porous	161° / N.A	none	51
	graphene, Si-NPs	thermal reduction	nano-sphere	157°/ N.A	none	52
	CNT	spray	nanotube	163° / 3°	glass, metal, etc.	53
	CNT, silicone elastomer	spray	nanopores	~ 154° / ~ 1°	Al. silicon	54
Metallic	AgCl, AuCl$_3$	electroless galvanic reaction	micro-nano topographical	~ 180° / N.A	copper	55
	NiCl·6H$_2$O, H$_3$BO$_3$, lauryl sodium sulfate	electrodeposition	micro-nano structure	> 160°/ < 1°	SS3162 sheet	56
	NiCl·6H$_2$O, CoCl$_2$·6H$_2$O, C$_2$H$_8$N$_2$. HCl, H$_3$BO$_3$	electrodeposition	hierarchical flower-like	167.3 ± 1.3°/ ~ 1°	AZ91D magnesium alloy	57
Metallic oxide	Ag, TiO$_2$	Plasma deposition	nanorods	~ 156° / N.A	Si(100) wafer	58
	Al	anodization	pyramids-on-pores	~ 155°/ ~ 0°	Al	59
	ZnSO$_4$ / Al(SO$_4$)$_3$ / FeSO$_4$·4H$_2$O	dip-coaring/ immerse	NPs	related to materials	sponge/fabric/paper	60
	FeSO$_4$·7H$_2$O, FeSO$_3$·6H$_2$O/FeO, Co(NO$_3$)$_2$·6H$_2$O/Ni(NO$_3$)$_2$·6H$_2$O/ Cu(CH$_3$CO$_2$)$_2$, CH$_3$COOH/AgNO$_3$	co-precipitation, immerse	micro-nano structure	N.A	textiles/sponges	61
organic polymer	AAO,PS	template method	long-neck vase-like	150.6° / N.A	PET	64
	LDPE, NH$_4$HCO$_3$	dip-coating	lotus-leaf-like	156 ± 1.7° / 1°	glass	65
	Aluminum,PP	microstructure technique and injection	fine-scale and micropillars	> 150° / < 5°	none	66
	Pentadecafluorooctanoyl chloride glycidyl methacrylate	ATRP	micro-nano structure	172° / N.A	bio-fiber	67

	DFMA, MMA, HEMA, BA	polymerization, spraying	porous	$164.1 \pm 1.7° / 2 \pm 0.4°$	Al	68
	chitosan, CF$_3$CF$_2$)$_7$SO$_3$Li	electrostaic reaction, spray	porous	$157.2 \pm 2.2°/ 14 \pm 5°$	cotton	69
	ZnO, PS	hydrothermal reaction, dip-coating	micro-nano structure	158° / N.A	cotton	70
organic-inorganic hybrid	PVDF-MWCNT	spray	porous	154° / < 3°	glass, Al	71
	TEOS, PEG	sol-gel	nanonetwork	168° / N.A	glass	72
	PU, MoS$_2$	spray	papillae-like	157° / N.A	various substrates	73

Table 2 A summary of the critique of various fabrication methods and materials in relation to the different applications

Application	Materials	Fabrication methods	Complexity	Durability	Cost	Ref
Oil-water separation	Copper meshes, silicone elastomer	CVD	Relatively simple	Fair	Inexpensive	166
	Graphene nanosheets, commercial sponge	Exfoliation and deposition	Complex	Good	Expensive	167
	Polyurethane sponges, methyltrichlorosilane	Solution immersion method	Simple	Good	Inexpensive	168
Corrosion resistance	Polystyrene, polythiophene	Electrodeposited	Relatively simple	Fair	Relatively inexpensive	179
	Tetraethyl orthosilicate , trimethylethoxysilane , methyltrimethoxysilane, hexadecyltrimethoxysilane	Sol–gel method	Simple	Fair	Relatively inexpensive	180
	Magnesium alloy MA8, methoxy-{3-[(2,2,3,3,4,4,5,5,6,6,7,7,8,8,8-pentadecafluorooctyl)oxy]propyl}-silane	Plasma electrolytic oxidation (PEO)	Complex	Good	Inexpensive	181
	Al$_2$O$_3$ nanoparticles，polyurethane	Suspension flame spraying	Relatively simple	Fair	Relatively inexpensive	160
Self-cleaning	High-density polyethylene，TiO$_2$ nanoparticles	Template lamination method	Relatively simple	Good	Inexpensive	194
	Anodized alumina oxide (AAO)，Silicon molds	Nanoimprinted	Relatively simple	Good	Inexpensive	195
	1H,1H,2H,2H	Etching and a coating	Simple	Good	Relatively	207

Category	Materials	Method	Complexity	Performance	Cost	Ref
	perfluorodecyltriethoxysilane [$CF_3(CF_2)_7CH_2CH_2Si(OC_2H_5)_3$, Aluminum plates				inexpensive	
Anti-icing	Uorinated acrylic copolymer	Spraying	Simple	Fair	Relatively expensive	68
	Multi-walled carbon nanotubes，Triton X-100，silicone elastomer	Deposition and spray	Complex	Good	Expensive	54
	Octamethylcyclotetrasiloxane,2,4,6,8-tetramethylcyclotetrasiloxane,1,1,3,3-tetramethyldisiloxane,1,1,3,3-tetramethyl-1, 3-divinyldisiloxane,	Polymerization	Complex	Good	Relatively expensive	208
Drag-reducing	Polydimethylsiloxane, Ti(OC_4H_9)$_4$,7075 aluminum alloy	Sol–gel method	Simple	Fair	Inexpensive	215
	Sylgard-184, polycaprolactone,Thermoplastic polyurethane,1,1,1,3,3,3-Hexamethyl disilazane, tetraethylorthosilicate	Sol–gel method	Simple	Fair	Inexpensive	216
	$HAuCl_4$, copper foil, n-dodecanethiol	Electroless deposition,CVD	Relatively simple	Fair	Expensive	217
Anti-bacteria	Isobutyltrimethoxysilane, methyltrimethoxysilane, (3-(4,5-dimethylthiazol-2-yl)-5-(3-carboxymethoxyphenyl)-2-(4-sulfophenyl)-2H-tetrazolium), phenazine methosulfate, tetraethylorthosilicate	Spray-coating	Relatively simple	Good	Relatively expensive	225
	Chitosan,cotton fabric	Spraying	Simple	Fair	Inexpensive	69
	$C_{12}H_{27}AlO_3$, silvernitrate, ethyl acetoacetate	Sol–gel method	Simple	Fair	Inexpensive	83
	$AgNO_3$, Hexadecyltrimethoxysilane, cotton textiles	Redox process,dipping	Relatively simple	Fair	Inexpensive	226
Transparency and anti-reflection	Polysiloxane, methyl-terminated poly(dimethylsiloxane)s	Solidification-induced phase separation method	Simple	Good	Relatively inexpensive	233
	Tetraethylorthosilicate ,	Sol gel dip-coating method	Simple	Good	Relatively	234

	γ-aminopropyltriethoxysilane				inexpensive	
	Poly(methyl methacrylate),	Dry etching,hydrolysis process	Complex	Good	Inexpensive	235

5

10

15

20

25

30

35

40

45

50